Intercomparison of global foliar trait maps reveals fundamental differences and limitations of upscaling approaches

Benjamin Dechant[1,2], Jens Kattge[3,1], Ryan Pavlick[4], Fabian D. Schneider[4], Francesco M. Sabatini[5,6], Alvaro Moreno-Martinez[7], Ethan E. Butler[8], Peter M. van Bodegom[9], Helena Vallicrosa[10,11,12], Teja Kattenborn[13,1], Coline C.F. Boonman[14], Nima Madani[15,4], Ian J. Wright[16,17], Ning Dong[18,19], Hannes Feilhauer[20,1], Josep Penuelas[11,12], Jordi Sardans[11,12], Jesus Aguirre-Gutierrez[21,22], Peter B. Reich[23,8,16] Pedro J. Leitão[20,1], Jeannine Cavender-Bares[24], Isla H. Myers-Smith[25], Sandra M. Duran[26], Holly Croft[27], I. Colin Prentice[18,28], Andreas Huth[29,30,1], Karin Rebel[31], Sönke Zaehle[3], Irena Simova[32,33], Sandra Diaz[34,35], Markus Reichstein[3,1], Christopher Schiller[36], Helge Bruelheide[37,1], Miguel Mahecha[20,1], Christian Wirth[38,3], Yadvinder Malhi[21,22], Philip A. Townsend[4,39]

Corresponding author: B. Dechant: benjamin.dechant@idiv.de

Twitter: @DechantBenjamin

THIS IS A NON-PEER REVIEWED PREPRINT SUBMITTED TO EARTHARXIV

[1] German Centre for Integrative Biodiversity Research (iDiv) Halle-Jena-Leipzig, Puschstr. 4, D-04103 Leipzig, Germany

[2] Leipzig University, Ritterstraße 26, 04109 Leipzig, Germany

[3] Max Planck Institute for Biogeochemistry, Hans Knöll Str. 10, 07745 Jena, Germany

[4] Jet Propulsion Laboratory, California Institute of Technology, 4800 Oak Grove Drive, Pasadena, CA 91109, USA.

[5] BIOME Lab, Department of Biological, Geological and Environmental Sciences (BiGeA), Alma Mater Studiorum University of Bologna, Via Irnerio 42, Bologna, 40126, Italy.

[6] Czech University of Life Sciences Prague, Faculty of Forestry and Wood Sciences, Kamýcká 129, 165 21 Praha Suchdol, Czech Republic

[7] Image Processing Laboratory (IPL), Universitat de Valéncia, Valencia, Spain

[8] Department of Forest Resources, University of Minnesota, 1530 Cleveland Ave N, St. Paul, MN 55108

[9] Institute of Environmental Sciences, Leiden University, Einsteinweg 2, 2333 CC Leiden, the Netherlands

[10] Department of Civil and Environmental Engineering, Massachusetts Institute of Technology, Cambridge, MA, USA

[11] CSIC, Global Ecology Unit CREAF-CSIC-UAB, Bellaterra, Barcelona 08913, Catalonia, Spain.

[12] CREAF, 08913 Cerdanyola del Vallès, Barcelona 08913, Catalonia, Spain.

[13] Department for Sensor-based Geoinformatics, Faculty of Environment and Natural Resources, University of Freiburg

[14] Center for Biodiversity Dynamics in a Changing World (BIOCHANGE) and Section for Ecoinformatics & Biodiversity, Department of Biology, Aarhus University, Ny Munkegade 114, 8000 Aarhus C, Denmark
[15] UCLA Joint Institute for Regional Earth System Science and Engineering. 4242 Young Hall, 607 Charles E. Young Drive East, Los Angeles, CA 90095, USA.
[16] Hawkesbury Institute for the Environment, Western Sydney University, Locked Bag 1797, Penrith, NSW 2751, Australia
[17] School of Natural Sciences, Macquarie University, NSW 2109, Australia
[18] Georgina Mace Centre for the Living Planet, Department of Life Sciences, Imperial College London, Silwood Park Campus, Buckhurst Road, Ascot, SL5 7PY, UK;
[19] Department of Biological Sciences, Macquarie University, North Ryde, NSW 2109, Australia.
[20] Remote Sensing Centre for Earth System Research (RSC4Earth), Leipzig University and Helmholtz Centre for Environmental Research, Talstr. 35, 04103 Leipzig, Germany
[21] Environmental Change Institute, School of Geography and the Environment, University of Oxford, Oxford, UK
[22] Leverhulme Centre for Nature Recovery, University of Oxford, Oxford OX13QY, UK
[23] Institute for Global Change Biology, and School for the Environment and Sustainability, University of Michigan, Ann Arbor, MI 48109, United States
[24] Department of Ecology, Evolution and Behavior, University of Minnesota, 1479 Gortner Ave., Saint Paul, MN 55108
[25] School of GeoSciences, University of Edinburgh, Edinburgh, EH9 3FF, UK
[26] Department of Forest and Rangeland Stewardship, Colorado State University, Fort Collins, Colorado, USA.
[27] School of Biosciences, University of Sheffield, Sheffield, S10 2TN, UK
[28] Ministry of Education Key Laboratory for Earth System modeling, Department of Earth System Science, Tsinghua University, Beijing 100084, China.
[29] Helmholtz Centre for Environmental Research - UFZ, Permoserstr. 15, 04318 Leipzig, Germany
[30] University of Osnabrück, Barbarastraße 12, 49076 Osnabrück, Germany
[31] Copernicus Institute of Sustainable Development, Environmental Sciences, Faculty of Geosciences, Utrecht University, Utrecht, The Netherlands;
[32] Center for Theoretical Study, Charles University, Husova 4, 110 00 Prague, Czech Republic
[33] Department of Ecology, Faculty of Science, Charles University, Viničná 7, 128 44 Prague, Czech Republic
[34] Consejo Nacional de investigaciones Científcas y Técnicas, Instituto Multidisciplinario de Biología Vegetal (IMBIV), Córdoba, Argentina
[35] Facultad de Ciencias Exactas, Físicas y Naturales, Universidad Nacional de Córdoba, Casilla de Correo 495, 4000, Córdoba, Argentina
[36] Institute of Geographical Sciences, Free University Berlin, Malteserstraße 74-100, 12249 Berlin
[37] Institute of Biology/Geobotany and Botanical Garden, Martin Luther University Halle-Wittenberg, Am Kirchtor 1, 06108, Halle, Germany
[38] Institute of Systematic Botany and Functional Biodiversity, Leipzig University, Leipzig, Germany.
[39] University of Wisconsin, Madison, WI, USA.

Highlights

- Analyses revealed two fundamentally different categories of upscaled trait maps
- Differences between categories mainly driven by use of plant functional types (PFTs)
- Additional differences due to whole community vs. top-of-canopy trait metrics
- Upscaling without PFTs does not capture the observed trait differences between them
- Accounting for within-grid-cell trait variation crucial for upscaling and evaluation

Graphical Abstract

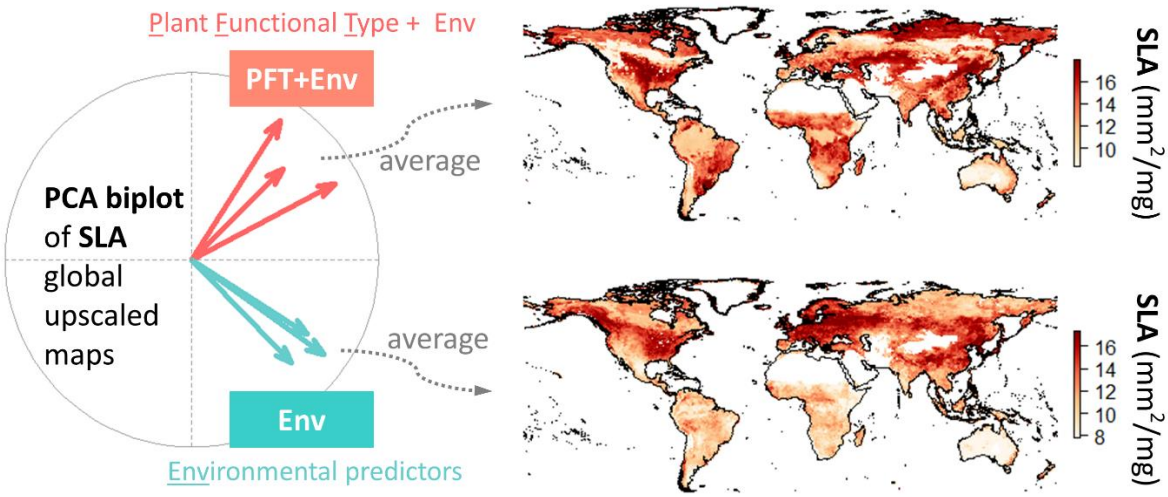

Abstract

Foliar traits such as specific leaf area (SLA), leaf nitrogen (N) and phosphorus (P) concentrations play an important role in plant economic strategies and ecosystem functioning. Various global maps of these foliar traits have been generated using statistical upscaling approaches based on in-situ trait observations.

Here, we intercompare such global upscaled foliar trait maps at 0.5° spatial resolution (six maps for SLA, five for N, three for P), categorize the upscaling approaches used to generate them, and evaluate the maps with trait estimates from a global database of vegetation plots (sPlotOpen). We disentangled the contributions from different plant functional types (PFTs) to the upscaled maps and characterized the differences between two trait metrics: community weighted mean (CWM) and top-of-canopy weighted mean (TWM).

We found that the global foliar trait maps of SLA and N differ drastically and fall into two groups that are almost uncorrelated (for P only maps from one group were available). The primary factor explaining the differences between these groups is the exclusive use of PFT information combined with remote sensing-derived land cover products in one group while the other group mostly relied on environmental predictors. The impact of using TWM or CWM on spatial patterns was considerably smaller than that of including PFT and land cover information. The maps that used PFT and land cover information exhibit considerable similarities in spatial patterns that are strongly driven by land cover. The maps not using PFTs show a lower level of similarity and tend to be strongly driven by individual environmental variables.

Overall, the maps using PFT and land cover information better reproduce the between-PFT trait differences and trait distributions of the *plot*-level sPlotOpen data, while the two groups performed similarly in capturing within-PFT trait variation. Upscaled maps of both groups were moderately correlated to *grid-cell*-level sPlotOpen data (R = 0.2-0.6), with considerable differences between upscaling approaches and overall higher correlations for SLA and N.

Our findings highlight the importance of explicitly accounting for within-grid-cell trait variation, which has important implications for applications using existing maps and future upscaling efforts.

Keywords: foliar trait, specific leaf area, leaf nitrogen, leaf phosphorus, global map, upscaling

1. Introduction

Vascular plants play a crucial role in the terrestrial Earth system due to their exchange of carbon, water, nutrients, and energy with the atmosphere and the pedosphere. Moreover, plants are important elements in the biosphere as they are strong drivers of the population dynamics of other organisms. Functional traits are important for characterizing vegetation function and plant ecological strategies related to metrics of performance, such as nutrient retention, biomass accumulation and CO_2 uptake (Bongers et al., 2021; Díaz et al., 2015; Wright et al., 2004). In particular, morphological and chemical leaf traits, such as specific leaf area (SLA) and leaf concentrations of phosphorus (P) and nitrogen (N), are key components of the leaf economic spectrum (Wright et al., 2004). In turn, the leaf economic spectrum contributes to determining plant growth strategies and canopy carbon exchange dynamics globally (Reich, 2014).

Due to their important roles in plant metabolism, the leaf traits N, P and SLA have been used as inputs to land surface models (Walker et al., 2017), but often in highly simplified ways. As there are currently no observations (or more direct estimates) of these key foliar traits at the global scale, most land surface modeling applications use plant functional type (PFT) look-up tables for key traits such as photosynthetic capacity, which is closely related with N, P and SLA (Kattge et al., 2009; Walker et al., 2014). These look-up tables contain PFT mean trait values that can be combined with remote sensing-based maps of land-cover types dominated by particular PFTs to approximate global trait distributions, but these approaches ignore large within-PFT trait variability driven by inter- and intraspecific trait variation (Kattge et al., 2011; Scheiter et al., 2013; Van Bodegom et al., 2012). Furthermore, the focus on dominant PFTs detectable by remote sensing emphasizes top-of-canopy vegetation and ignores the complexity of multi-layered ecosystems.

To overcome the limitations of simplified approaches based on PFT mean trait values for land surface modeling applications and to address ecological questions (related to aspects of functional biodiversity), static maps of SLA, N, P and other traits have been produced based on *in-situ*, leaf-level trait measurements using statistical upscaling approaches at regional (Loozen et al., 2020; Šímová et al., 2018; Swenson and Weiser, 2010; Zhang et al., 2021) and global scales (Boonman et al., 2020; Butler et al., 2017; Madani et al., 2018; Moreno-Martínez et al., 2018; Schiller et al., 2021; Vallicrosa et al., 2021; van Bodegom et al., 2014; Wolf et al.,

2022). These upscaled maps of N, P and SLA were generated using different methods, different trait databases and were developed for a range of purposes, such as supporting land surface modeling, biodiversity characterization or a trait-based estimation of the distribution of vegetation types. Given these contrasting approaches and aims, we sought to understand the degree of consistency among these maps, as well as their performance when evaluated in comparison to *in-situ* data.

For potential users, the reliability of upscaled global foliar trait maps and their suitability for specific purposes are difficult to assess. Identifying the key sources of uncertainties and limitations of these maps can provide guidance for users and help improve global mapping of plant traits. Here we provide a comprehensive evaluation of the current global upscaled foliar trait maps of SLA, leaf nitrogen concentration (N) and leaf phosphorus concentration (P) consisting of the following elements:

1) Categorization of upscaling approaches;
2) Comparison of spatial patterns and attribution of differences to upscaling methodology;
3) Evaluation against trait estimates based on a global vegetation plot database.

2. Materials and methods

2.1 Terminology

The upscaling of foliar trait maps is relevant for different scientific communities (e.g., land surface modeling, vegetation remote sensing, macroecology), which may use different terms or partly similar terms that have different meanings. To avoid misunderstandings and be able to use convenient shorthand notations for concepts frequently used throughout the manuscript, we clarify our use of key terms with the following definitions (Table 1). We do not claim that these definitions are necessarily optimal or universal, rather, they serve as a pragmatic way to clarify terms used in the presentation of our study. Note that the land cover types (LCTs) we consider are land cover *functional* types in the sense that they can be directly matched to PFTs (Table 1) in the sense used in previous work (Friedl et al., 2002; Poulter et al., 2015). We use the more general term ´PFT information´ to include both (in-situ) PFT and (grid-cell-level) LCT for the sake of convenience as PFT and LCT data were typically used together in the upscaling.

Table 1: Glossary of terms.

Plant functional type (PFT)	classification of plants, mostly based on growth form, leaf type and leaf phenology. Example: evergreen needleleaf tree.
Land cover type (LCT)	remote sensing-based classification of the land cover, dominated by specific PFTs. Example: evergreen needleleaf forest.
Community weighted mean (CWM)	the mean trait value of a community weighted by the species cover, abundance, or biomass. In the case of the sPlotOpen dataset the weighting is done by species cover or abundance.
Top-of-canopy weighted mean (TWM)	the mean trait value at the top-of-canopy weighted by the cover of the species that constitute the dominant PFT of a plot.
Homogeneous grid cells	grid cells with low trait variability, either occupied by a single LCT or several LCTs with similar trait values.
Heterogeneous grid cells	grid cells with high trait variability, occupied by more than one dominant PFT with notable differences in mean trait values of the dominant PFTs.

2.2 Trait maps

We identified seven publications in the literature (state June 2022) that present global, statistically upscaled trait maps with at least one of the three traits SLA, N or P: van Bodegom *et al.* (2014); Butler *et al.* (2017); Madani *et al.* (2018), Moreno-Martínez *et al.* (2018), Boonman *et al.* (2020), Schiller *et al.* (2021), and Vallicrosa et al. (2021) (Table 2). For the sake of simplicity, we use a short version of the last name of the first author of each map-related publication to refer to the different maps, e.g., 'Bodegom' refers to the map of van Bodegom et al. (2014). 'Moreno' refers to Moreno-Martinez et al. (2018) (see Table 2).

The degree of completeness of the spatial coverage of the maps differed. Four maps provided gap-free global maps (Bodegom, Butler, Madani, Boonman), while the two high-resolution maps excluded cropland (Moreno, Vallicrosa). Schiller had gaps in different regions due to the availability/selection of plant photographs from iNaturalist. All upscaling approaches except Madani only considered trait variation in natural vegetation and excluded foliar traits in croplands. This implies that trait values in cropland areas indicate traits of natural vegetation actually or potentially occurring there. While most approaches considered vegetation of different growth forms, Vallicrosa only mapped traits for woody vegetation (Table 2).

Table 2: Overview of of the seven upscaling approaches and the corresponding maps. Note that PFT use also implies use of land cover type products.

Lead author	Year	Traits	PFT use	Reso-lution†	Vegetation Considered	Reference
Bodegom	2014	SLA	no	0.5 °	Natural‡	van Bodegom et al. (2014)
Butler	2017	SLA, N, P	yes	0.5 °	Natural‡	Butler et al. (2017)
Madani	2018	SLA	yes	0.05 °	All	Madani et al. (2018)
Moreno	2018	SLA, N, P	yes	0.008 °	Natural*	Moreno-Martínez et al. (2018)
Boonman	2020	SLA, N, P	no	0.5 °	Natural‡	Boonman et al. (2020)
Vallicrosa	2021	N, P	yes	0.008 °	Woody	Vallicrosa et al. (2021)
Schiller	2021	SLA, N	no	0.5 °	Natural‡	Schiller et al. (2021)

† The resolutions 0.5°, 0.05°, and 0.008° correspond to square grid cell sizes of about 50 km, 5 km and 1 km at the equator.

‡ No crop traits in training data but predictions for cropland areas, corresponding to potential natural vegetation.

* No crop traits in training data and no predictions for cropland areas.

2.3 Upscaling approaches

All approaches derived gridded global trait maps from globally distributed leaf-level *in-situ* observations (Fig. S1) and upscaling approaches can be characterized by two steps of upscaling: (1) leaf-to-grid scaling, i.e. the scaling of in-situ leaf-level data to the respective cells of a spatial grid, and (2) spatialization, i.e., increasing the spatial coverage from the limited number of grid cells with *in-situ* data to the global land surface (Fig. 1). All approaches except Schiller applied step (1) before step (2) (Fig. 1) and applied regression-based spatialization that first established trait-environment relationships for the reference grid cells and then applied them to the global vegetated land surface to obtain global maps. Schiller, however, switched the order of the two upscaling steps and first estimated trait values for a large number of iNaturalist photographs of individual plants distributed globally and aggregated these trait values to grid-cell-level in the second step.

There were important differences between the upscaling approaches in essentially all aspects of the upscaling processing chain (Fig. 1). The approaches differed in their motivations, input data and its processing, leaf to grid scaling methods, and spatialization including both the choice of predictor variables and regression algorithms (Fig. 1, Text S1 in the supplementary material). The environmental predictors used in the upscaling approaches were mainly related to temperature, solar radiation, water availability and soil characteristics (Table S1) and came from a variety of climate and soil products (Table S2). Importantly, there were differences

whether and how PFT and LCT information was used for upscaling (Fig. 1). Moreno was the only approach that directly used optical reflectance satellite remote sensing data as predictors in the spatialization (Table S1).

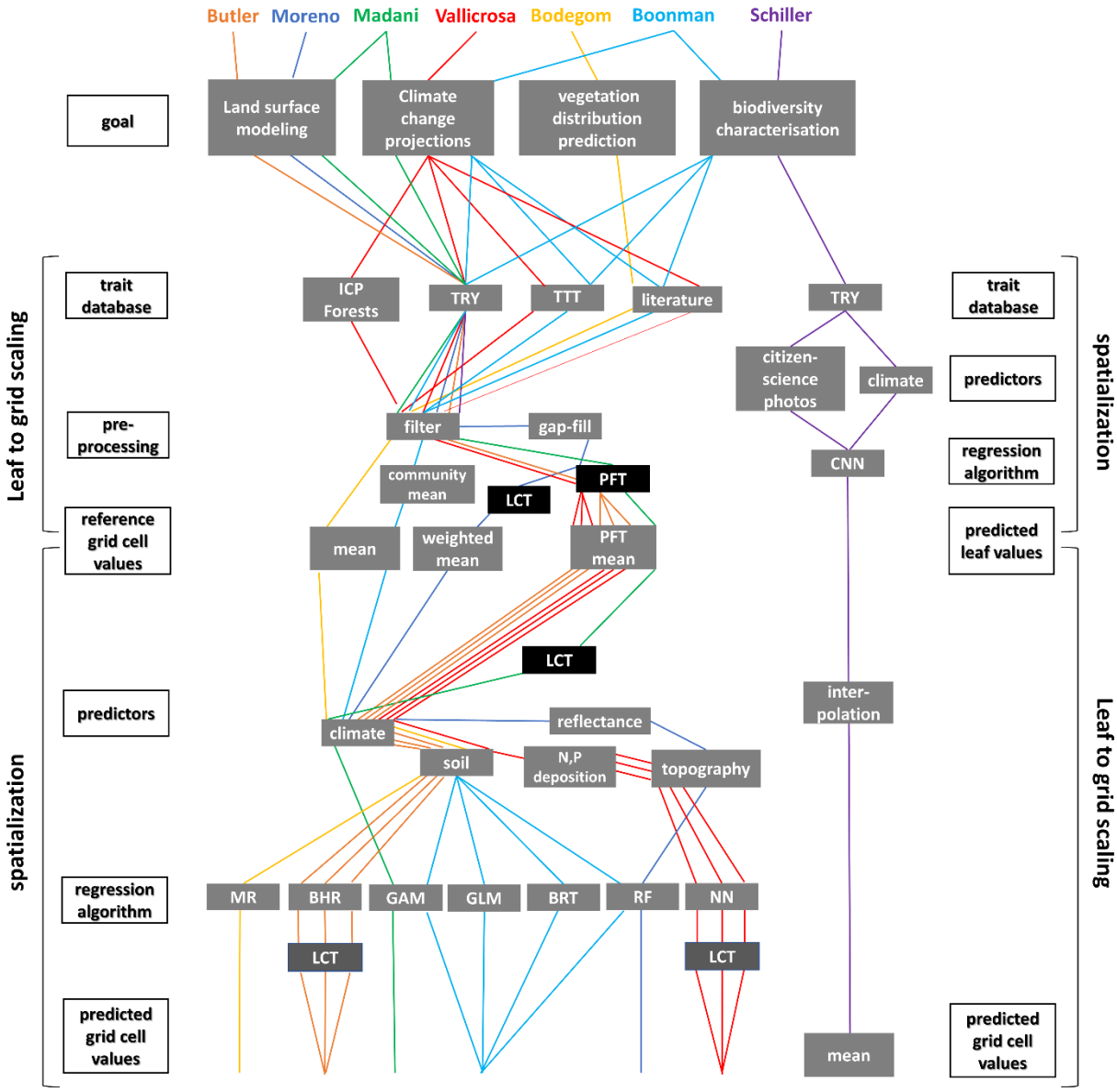

Figure 1: Schematic overview of the seven upscaling approaches. Each upscaling approach is shown in a separate color. Special emphasis is put on the use of plant functional type (PFT) and land cover type (LCT) information shown in dark grey color. The explanatory column on the left hand side applies to all approaches except Schiller for which the corresponding column on the right hand side applies. 'TTT' refers to the Tundra Trait Team database, 'literature' to data based on individual publications. The regression algorithms include multiple linear regression (MR), Bayesian hierarchical regression (BHR), generalized additive models (GAM), generalized linear models (GLM), generalized boosted models (GBM), random forests (RF), neural networks (NN), convolutional neural networks (CNN).

Categorization of upscaling strategies. All maps used environmental predictor information ('Env') in the spatialization step but only some used PFT information. Therefore, we use the shorthand notation of 'PFT+Env' vs. 'Env' maps to more generally distinguish the upscaling approaches that used PFT information from those that did not. Note that there are considerable differences in the way PFT information was used in the PFT+Env approaches. Also, the Schiller map is categorized as 'Env' upscaling approach for the sake of convenience (Fig. 1), although information from ground-based RGB images was used in addition to environmental drivers.

Additional versions of the Butler and Moreno maps. To quantify the relative contributions of different types of predictor information to the upscaled trait maps, we also analyzed versions of the Butler and Moreno trait maps that differed only in the predictor variables used. This allows for a direct comparison of PFT+Env, PFT, and Env maps (Butler) based on identical input data and regression algorithms as well as quantifying the impacts of the remote sensing predictors (Moreno). Note that the ´PFT´ maps only using fixed trait values per LCT are referred to as categorical maps in Butler et al. (2017). We also make use of this term (categorical) in the text to avoid potential confusion of ´PFT´ trait maps with maps of PFT cover that would correspond to LCT maps. The Butler (original) categorical maps were based on LCT-specific mean values of relevant data in the TRY database and therefore might not be optimal regarding the comparison with the full PFT+Env maps. To quantify to what degree categorical maps could capture the patterns of the full PFT+Env maps in the ideal case, we adjusted the mean trait values per LCT to better capture the latitudinal patterns of the PFT+Env maps, which resulted in a stronger correlation, especially for SLA and P (Fig. S2). The maps with these adjusted values are referred to as optimal categorical maps and are used in the main analyses to focus on the differences due to within LCT trait variation rather than differences in the mean LCT trait values.

2.4 Data processing

2.4.1 Global foliar trait maps

We used global trait maps provided by the map developers (the leading authors of the relevant publications) to ensure that we had the most up-to-date and correct versions of the upscaling

products. A list of the sources is provided in the supplementary material (Table S3). We only used maps representing the present and recent past and did not consider maps of future change predictions such as Madani et al. (2018). We aggregated the higher resolution maps (Madani, Moreno, Vallicrosa) to the common resolution of 0.5 degree using the Bodegom map as reference regarding the projection and coordinate origin. For this, we used the *aggregate* function of the *raster* package in R (Hijmans, 2022) and averaged over all available high resolution grid cells within a coarse grid cell ignoring missing-data and zero values. Non-vegetated grid cells such as bare soil, ice/snow etc. were excluded by selecting grid cells with a minimum vegetation cover of of 5% based on the LCT map used by Butler. Madani was the only data set to provide estimates for croplands, so prior to aggregating to 0.5°, we masked out the cropland grid cells at the original resolution of 0.05° using the land cover map used by Madani. We did not mask out cropland-dominated grid cells at 0.5° to include the trait variation of (potential) natural vegetation in cropland regions.

2.4.2 Separation of land cover - driven and environmentally driven trait variation and stratification by PFT

Our initial analyses revealed that LCT-driven trait variation dominated the global spatial trait patterns of the PFT+Env maps. As one objective of the upscaling approaches was estimating trait variation within PFTs, it is important to disentangle the dominant LCT-driven trait variation that is related to *between*-PFT trait variation from the variation *within* PFTs. The common approach to quantify variations within LCTs is to select only homogeneous grid cells by applying a threshold on the cover fractions of LCTs. However, this approach has an important limitation: the LCT cover threshold only considers the homogeneity in land cover but not the variation of foliar traits, which we aim to quantify. Therefore, we estimated the trait heterogeneity based on fractional LCT using PFT mean trait values. We found that the relationship between land cover homogeneity and trait homogeneity can be complex, partly showing even a strong negative relationship (Fig. A1b in Appendix A). This implies that in addition to a threshold on the cover fraction of LCTs, a second threshold on the homogeneity in traits is needed. This double threshold approach ('heterogeneity filtering'), resulted in a reasonable number of homogeneous grid cells for three of the six LCTs, but for the remaining three not enough grid cells remain (Figs. A1c in the Appendix). Therefore, we developed a complementary second approach to unmix LCTs in heterogeneous grid cells. For analyses at the level of PFTs/LCTs (Figs. 4b, 7, A2c, S7, S8, S10, S12, S13) we combined the two

approaches to obtain sufficient data for all LCTs. Both approaches are described in more detail in Appendix A. Deciduous needleleaf forest (DNF) was excluded from further analyses due to the sparseness of in-situ reference data and the limited geographic extent of the distribution compared to the other LCTs: evergreen broadleaf forest (EBF), evergreen needleleaf forest (ENF), deciduous broadleaf forest (DBF), shrubland (SHR) and grassland (GRA).

2.4.3 Evaluation against sPlotOpen

To evaluate the upscaled maps against data not directly used in the upscaling, we used the sPlotOpen database (Sabatini et al., 2021). sPlotOpen is an open-access collection of 95,104 vegetation plots sampled in the field, spanning 114 countries. It consists of a stratified random selection of vegetation plots derived from sPlot - The Global Vegetation plot database (Bruelheide et al., 2019). Plots vary widely in size, ranging between 0.03 and 40,000 m^2. For each plot, sPlotOpen reports the list of vascular plant species, together with a measure of their relative abundance. Species mean trait values, as extracted from the TRY database (Kattge et al., 2020, 2011), were combined with species abundance data to calculate plot-level community weighted mean (CWM) trait values. To evaluate the impact of vertical variations of foliar traits due to species composition, we calculated top-of-canopy weight mean (TWM) trait estimates per plot, in addition to the standard CWM trait estimates, which integrate traits from all vegetation layers. This was done by first determining the dominant PFT of each plot using thresholds on the species cover of a given PFT (Table S4) and then calculating the weighted mean over all species of the dominant PFT of the plot. One motivation to conduct the CWM vs. TWM comparison were the differences in upscaling approaches regarding the scaling from leaf to the grid cell. To compare sPlotOpen and upscaled maps at the level of individual PFTs, we stratified both CWM and TWM by PFT by using the dominant PFT of the plot. We used the six PFT categories defined above (ENF, DNF, EBF, DBF, SHR, GRA) and matched the species in sPlotOpen to these categories using plant growth form, leaf type and leaf phenology type from the TRY database and literature.

We compared characteristics of the upscaled maps with sPlotOpen at two levels: using *plot*-level sPlotOpen data and *grid-cell*-level sPlotOpen data (Fig. S3a).

For a grid-cell-level comparison, the sPlotOpen plot data has to be scaled to the grid cell given the fact that sPlotOpen plots are much smaller than the typical grid cell size (50 km) of global upscaled trait maps. This was done as follows to ensure direct comparability to the upscaled

maps. For the comparison to Env upscaled maps, we aggregated the plot-level CWMs to the 0.5° grid cells without any weighting. For the comparison to PFT+Env upscaled maps, for each PFT, we first aggregated the plot-level TWM data to the 0.5° grid cells without weighting and then combined the six sPlotOpen PFT maps per trait by applying a weighted average based on the fractional LCT cover for each 0.5° grid cell. Data filtering was applied to ensure that sufficient data from sPlotOpen was available to be reasonably representative of a grid cell by applying a 99% threshold on the cumulated LCT cover. The high threshold is necessary as small fractions of missing coverage can considerably impact the result if the missing PFT has a very different trait value compared to the other PFTs that are represented, e.g. ENF (Fig. A1b). Also, outliers in the sPlotOpen data were removed by applying a 90^{th} percentile threshold for each trait. For the comparison of between- and within-PFT trait variation we used unweighted grid-cell averages of all relevant plots per PFT (with the partial exception of plot-level data in Figs. 8c, S11). To better visualize spatial patterns of global maps, we calculated latitudinal median values by averaging over latitudinal intervals and ignoring missing values.

A cross comparison of leaf-to-grid scaling approaches not matching the approaches of the upscaled maps was also included to quantify the impact of such a mismatch on the results.

2.5 Statistical analyses

Principal component analysis (PCA) was used to visualize the grouping and relative correlation of different trait maps. Variables were centered and scaled to unit variance for PCA using the *prcomp* function in base R. Pearson correlation (R) was used to quantify the similarity between two given maps. Apart from the 'normal' correlation based on all selected grid cells, we also quantified the degree of 'local correlation' by calculating correlations in a moving window of 3 × 3 grid cells to quantify the similarity in spatial patterns at smaller scales using the *corLocal* function of the *raster* package (Hijmans, 2022). For each pair of maps, the local correlation produces a correlation map and to summarize that map, the median was calculated.

All analyses and image processing were conducted using R version 4.0.2 (R Core Team, 2012), primarily with the *raster* package (Hijmans, 2022).

3. Results

3.1 Intercomparison of global maps and attribution of differences

3.1.1 Grouping of maps according to spatial patterns

A visual comparison of the different maps for SLA, N and P indicated striking differences between the maps for each trait but no obvious grouping or similarities at first sight (Figure B1 in the Appendix). However, we found that the maps of SLA and N both clustered according to the use of PFT and LCT information for the upscaling of *in-situ* trait information: approaches using this additional information ('PFT+Env') were similar among each other and different from the other approaches that mostly used only environmental predictors ('Env') (Fig. 2a). The first two axes of the PCA explained 60%-65% of the variance. The patterns in the PCA biplots were confirmed by pairwise correlation analyses showing a higher degree of within-group correlations for the approaches that used PFT information (Fig. 2b). The local correlations were moderately strong for the PFT+Env category but were zero for the Env category. High local correlations between maps from the PFT+Env group coincided with grid cells of high within-cell trait heterogeneity (results not shown). For N, the PCA results were generally similar as for SLA (Fig. 2a) although one of the two Env maps did not fall into either group and showed low correlations to all other maps. The first two axes of the PCA explained 50%-60% of the variance. For P, only maps based on the use of PFT information were available. They showed similar global pairwise correlations as for SLA, but higher values for the homogeneous grid cells and slightly lower local correlation when all or the heterogeneous grid cells were selected (Fig. 2b).

The strong separation of SLA and N maps was mostly due to the impact of using fractional LCT information rather than potential differences in the trait-environment relationships. This is supported by two separate analyses. First, 'PFT' maps that only used fractional LCT combined with fixed trait values per LCT fell into the same group of maps as the PFT+Env maps (Figs. S5c). Second, results for only the heterogeneous grid cells (Fig. S4a) showed consistent (SLA) or even stronger (N) separation of groups as the results for all grid cells (Fig. 2a). The interpretation based of the heterogeneity filtering results is complicated by the much higher heterogeneity levels of some of the LCTs (Fig. A1c) but this has a stronger impact on the selection of homogeneous than heterogeneous grid cells.

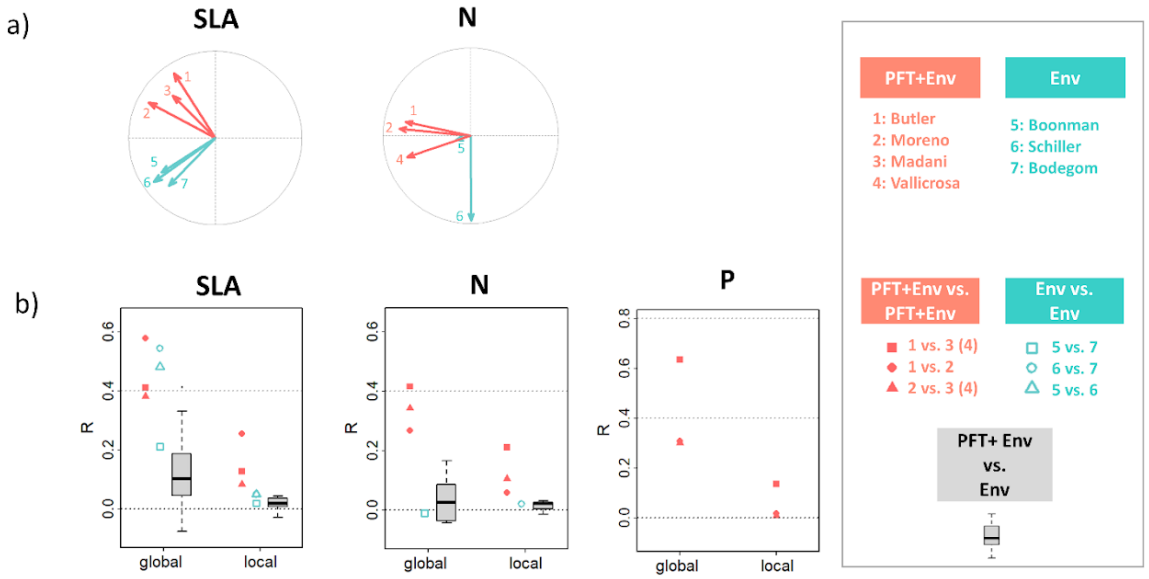

Figure 2: Overview of principal component analyses and pairwise correlation of upscaled maps for specific leaf area (SLA), leaf nitrogen (N) and phosphorus (P) concentration. In the principal component biplots with the first two axes a) and the pairwise correlation plots b), colors correspond to the use of predictor variables ('Env' stands for environmental variables, while 'PFT' stands for plant functional type and land cover type information). Pearson correlation is shown either for all selected grid cells ('global') or as median value of the local spatial correlation map in 3 x 3 pixel windows ('local'). In b) the gray boxplots contain all possible pairs of PFT+Env maps and the Env maps; for the PFT+Env maps, the same symbols are used for the cases 'x vs. 3' and 'x vs. 4', as 3 is only available for SLA and 4 only for N and P; note that the symbols for P and the case '1 vs. 2' and '2 vs. 4' are so close that they are hard to distinguish visually.

3.1.2 Spatial patterns: between and within-group differences

We grouped the maps according to their use of PFT information and calculated the trait averages over all maps within a given category as well as the coefficient of variation (CV) for each grid cell as a metric for dissimilarity (Fig. 3). These 'synthesis maps' and corresponding CV maps of SLA and N differed strongly between the PFT+Env and Env groups (Fig. 3). On average, the CV values within the PFT+Env group were lower than in the Env group. Despite the higher level of similarity of the PFT+Env maps compared to the Env maps, there were notable differences between individual PFT+Env maps of all three traits such as the much higher trait values of the Butler maps at high latitudes (Fig. B1 in Appendix B).

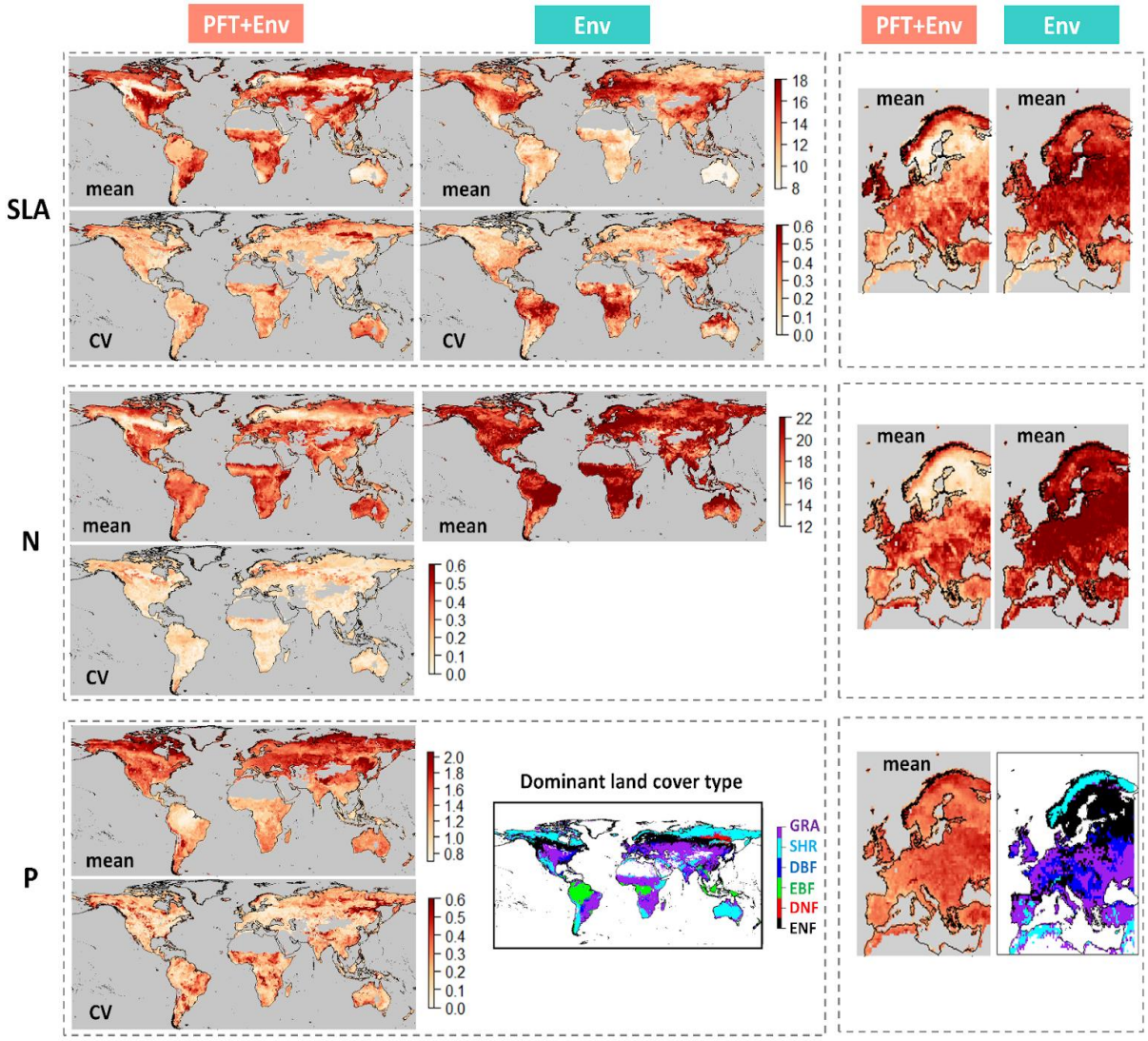

Figure 3: Overview of spatial patterns of specific leaf area (SLA, mm^2/mg), leaf nitrogen (N, mg/g) and phosphorus (P, mg/g) for different upscaled maps. For each trait, the the upper row shows the average and the lower row shows the coefficient of variation (CV) between the maps of each upscaling category: those that used both plant functional type and environmental information (PFT+Env) and those that use mostly only environmental predictors (Env). The average trait maps for Europe are shown besides the global maps and have the same color scales as the corresponding global maps. The global and European maps of dominant land cover type are shown for reference (ENF: evergreen needleleaf forest; DNF: deciduous needleleaf forest; EBF: evergreen broadleaf forest; DBF: deciduous broadleaf forest; SHR: shrubland; GRA: grassland).

In contrast to the average Env maps, the average PFT+Env maps showed a close correspondence between spatial patterns of traits and land cover (Fig. 3, 4a). For SLA, the PFT+Env mean map had high values in regions dominated by GRA, and SHR PFTs and a distinct band of low values for ENF (Figs. 3, 4a). The Env mean map, in contrast, showed overall low values in the Southern Hemisphere and a band of higher values in parts of the Northern Hemisphere dominated by GRA and ENF (Figs. 3, 4a). For N, the PFT+Env mean map showed somewhat similar patterns with a band of low values in the ENF dominated areas, while the Env mean map had overall high values with little contrast between the Northern and Southern Hemispheres. Also when looking at Europe in more detail (Fig. 3), the PFT+Env maps for SLA and N showed spatial patterns corresponding to dominant LCTs while the Env maps showed little contrast between dominant LCTs. For P, the mean PFT+Env map showed the lowest values in EBF-dominated regions and clearly lower values in the Southern than the Northern Hemisphere. P had somewhat lower values in the ENF-dominated region compared to the surrounding areas but the contrast was smaller than for SLA and N.

The higher level of similarity in spatial patterns within the PFT+Env category compared to the Env category was also visible in the latitudinal median patterns of the individual maps (Fig. S6). In particular, the PFT+Env maps showed strongly covarying latitudinal patterns for all three traits despite offsets in absolute values for SLA and divergence at the high northern latitude while Env maps showed very different patterns (Fig. S6). For N, PFT+Env maps showed consistent latitudinal patterns above 25 degree south and divergent patterns below, while Env maps showed the opposite tendency.

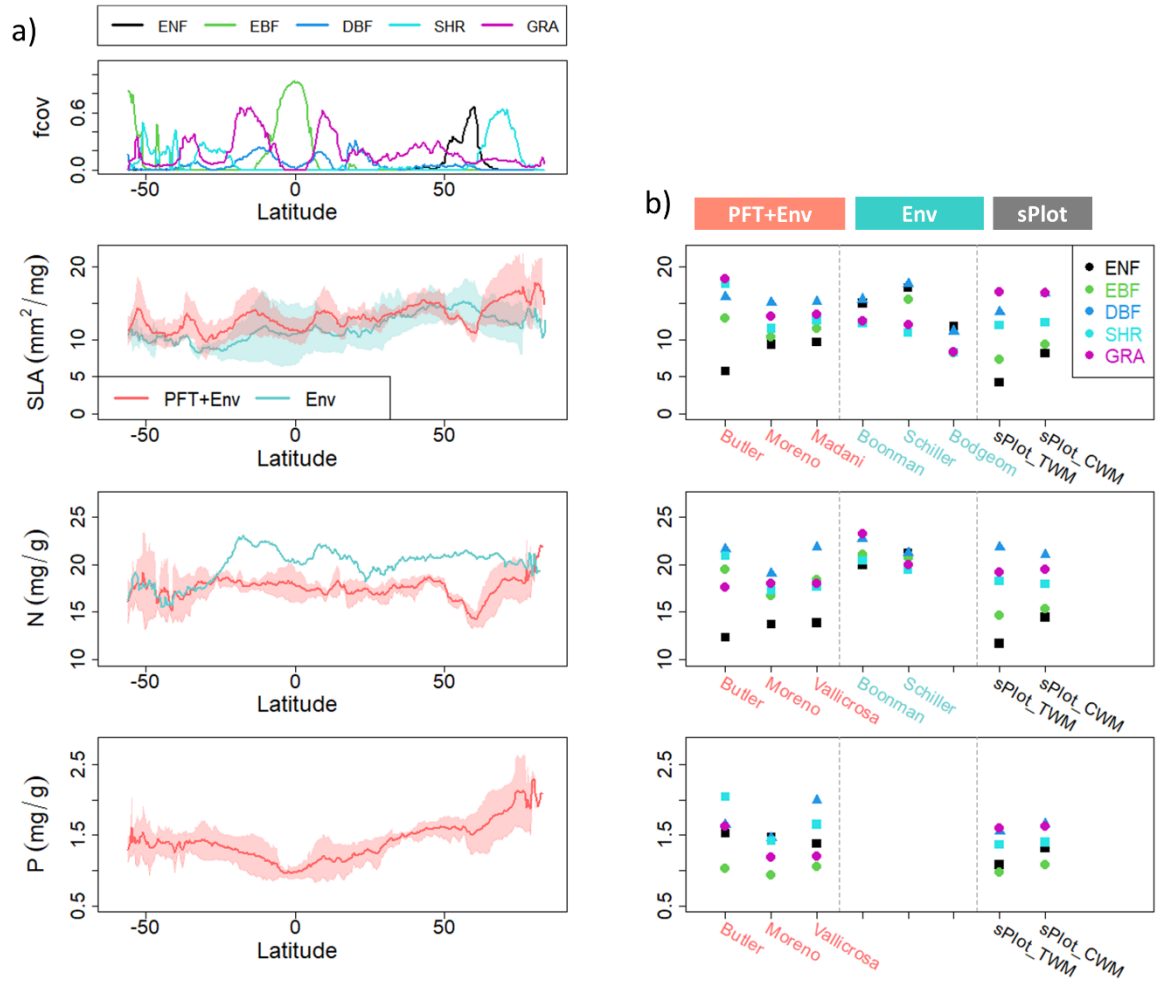

Figure 4: Latitudinal patterns of upscaled trait maps and differences between plant functional types (PFTs). a) Median latitudinal trait values of fractional PFT cover (fcov) and median latitudinal trait values of specific leaf area (SLA), leaf nitrogen (N) and phosphorus contents (P) averaged over the two upscaling groups (PFT+Env vs. Env). The shading around the mean values indicates one standard deviation in cases where there were at least three maps. b) Comparison of mean PFT (fcov > 0.5) trait values per upscaling approach with colors indicating each PFT (ENF: evergreen needleleaf forest; EBF: evergreen broadleaf forest; DBF: deciduous broadleaf forest; SHR: shrubland; GRA: grassland). TWM indicates top-of-canopy weighted mean, and CWM includes all vertical layers (see Table 1).

3.2 Evaluation of upscaled global trait maps with sPlotOpen

3.2.1 Comparison to sPlotOpen plot-level data

Latitudinal median values. When selecting only the grid cells from upscaled maps for which sPlotOpen data is available, we found some agreement in the latitudinal patterns of upscaled maps and sPlotOpen plot data (Fig. S9). In particular, the average of the PFT+Env maps agreed well with sPlotOpen data for SLA, N and P in the northern hemisphere including the lower values for ENF (Fig. S9). The latitudinal mean patterns of sPlotOpen trait data only showed rather small differences between TWM and CWM (Fig. S9).

Latitudinal distributions. While latitudinal mean or median values can be a useful way to summarize global patterns and compare absolute values, they cannot capture the complexity of multi-modal trait distributions well. The full latitudinal trait distributions of upscaled maps showed considerable differences compared to sPlotOpen plot data (Fig. 5). Also, there were large differences between CWM and TWM distributions, with TWM showing a tendency to broad, multi-modal distributions and CWM a tendency to narrower, unimodal distributions (Fig. 5).

Some of the PFT+Env maps showed considerable similarities with the sPlotOpen TWM distributions with a higher level of agreement for SLA than for N and P (Fig. 5). For SLA, the Butler map best captured the latitudinal patterns of the TWM distribution peaks including the double peak feature in the higher northern latitudes. This double peak feature was also partly captured by the Moreno and Madani maps but with a smaller distance between the peak in case of Moreno and a much lower secondary peak in case of Madani. While the Butler and Madani upscaled maps at least partly captured the lower trait values of sPlotOpen TWM at higher latitudes, they did not capture the higher values that also contributed to the overall wider distributions (Fig. 5). For N, PFT+Env upscaled maps did not capture the wide distributions of sPlotOpen TWM in the tropics well. Also, the overall latitudinal patterns of the peaks of the distributions were less consistent between upscaled maps and sPlotOpen TWM than for SLA. For P, the overall latitudinal patterns of PFT+Env upscaled maps was similar to sPlotOpen TWM, but Butler and Moreno maps had considerably narrower distributions than Vallicrosa and sPlotOpen TWM.

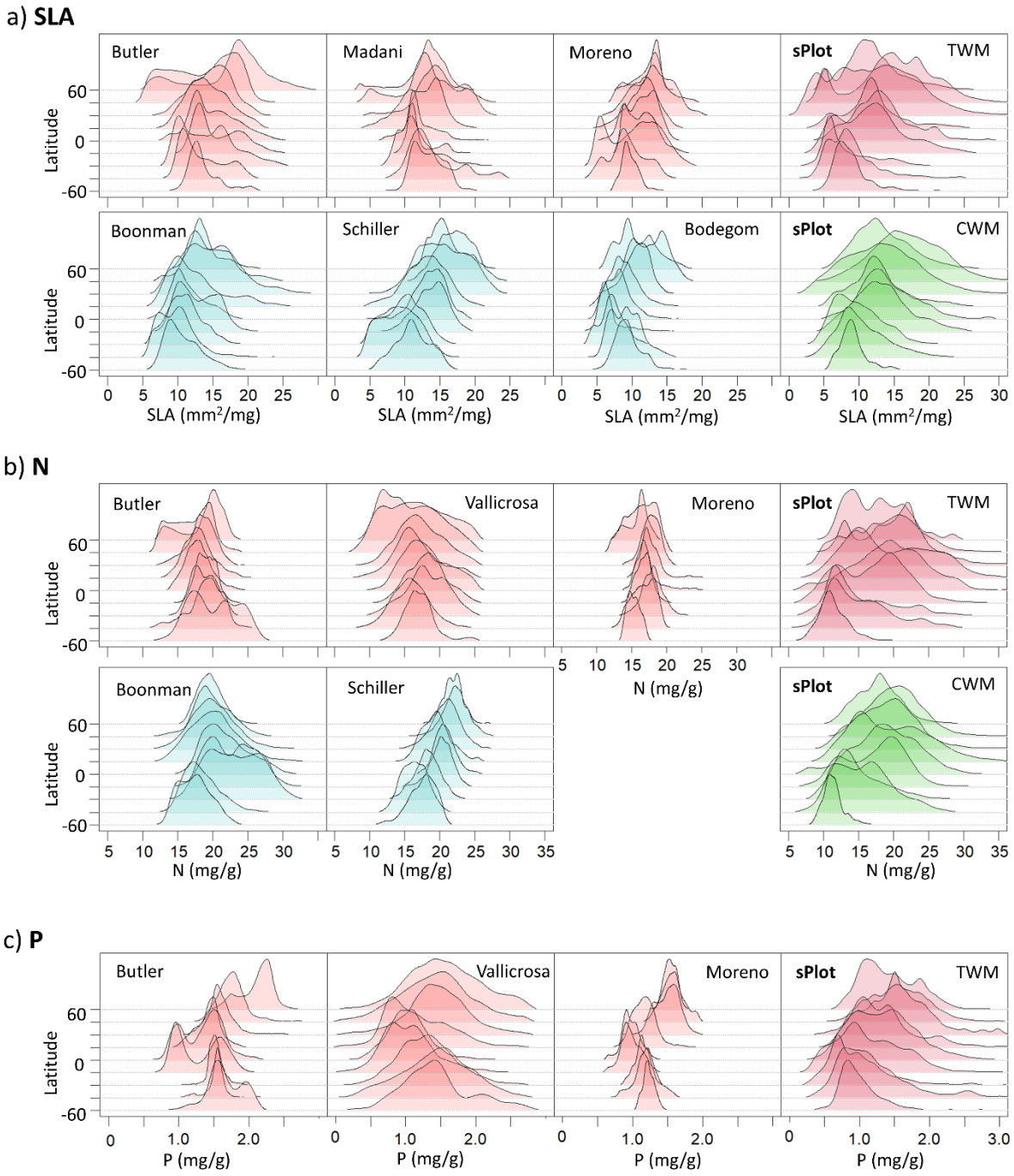

Figure 5: Latitudinal trait distributions for specific leaf area (SLA, mm^2/mg), leaf nitrogen (N, mg/g) and phosphorus (P, mg/g) of upscaled maps and sPlotOpen plot-level data. For each trait, the distributions in latitude intervals (units in degrees) are shown, with the upscaling approaches using plant functional type, land cover and environmental information (PFT+Env) in the top row in red color, and those mostly relying only on environmental information (Env) in the bottom row. Plot-level sPlotOpen ('sPlot') top-of-canopy weighted mean (TWM) are compared to the PFT+Env maps and community weighted mean (CWM) to the Env maps.

Some of the Env upscaled maps showed considerable similarities to the latitudinal distributions of sPlotOpen CWM also with a higher level of similarities for SLA than for N (Fig. 5). For SLA, the Schiller map best captured the patterns in the sPlotOpen CWM data, with general agreement in the patterns of latitudinal peaks. However, neither the Schiller nor the Boonman and Bodegom maps captured the broader distribution of sPlotOpen CWM due to the increasing presence of lower trait values in the higher northern latitudes. For N, the Schiller map agreed better with sPlotOpen CWM than the Boonman map when focusing on the overall decrease in the peak N values towards higher latitudes. However, the patterns of broader and partly double peaked distributions of sPlotOpen CWM were not captured by the Schiller map that had narrow, unimodal distributions across the entire latitudinal range. The Boonman map better captured the double peaked distribution of sPlotOpen CWM in the southern hemisphere but showed a decreasing trend towards the higher latitudes.

3.2.2 Comparison to sPlotOpen data scaled to the grid level

With PFT stratification

We found large differences between upscaled maps regarding both the spread of trait values between PFTs and the absolute values (Fig. 4b). A general tendency was that the PFT+Env maps showed larger spread between PFTs than the Env maps. This larger spread of the PFT+Env maps was more consistent with grid-level sPlotOpen data for SLA and N than for the Env maps even when considering the difference between TWM vs. CWM. While CWM showed smaller between-PFT differences than TWM, they were still clearly visible and had mostly similar patterns between PFTs (Fig. 4b). The description of results focuses on mean PFT trait values for the sake of simplicity, but the differences in spread between PFTs can also be observed across latitudinal gradients (Figs. S7, S8).

For SLA, only the Butler map had a similar level of spread between PFTs as sPlotOpen TWM and was the only map that came close to matching the low values for ENF (Fig. 4b). However, the Butler map had much higher values for SHR than sPlotOpen and EBF was also considerably higher but these discrepancies were due to specific latitudinal ranges and agreement in others was considerably better (Fig. S8). The other two PFT+Env maps (Moreno, Madani) were more consistent with sPlotOpen in terms of the order of PFTs, but had considerably smaller between-PFT differences (even smaller than for CWM). While the Env maps differed somewhat in the absolute values, they generally tended to have the highest values

for ENF and the lowest values for SHR and GRA, which was opposed to the patterns in sPlotOpen CWM (Fig. 4b).

For N, the difference in values for ENF among the PFT+Env maps was smaller than for SLA, but the differences in spread between PFTs and the order of PFTs were still considerable (Fig. 4b). Similar to SLA, Butler showed higher values for SHR and EBF than sPlotOpen TWM and showed more similar values for DBF and GRA. As for SLA, Moreno showed a similar order of PFTs as sPlotOpen but even smaller spread than CWM. The Vallicrosa maps showed large differences between ENF and DBF but very similar values for the other PFTs. The two Env maps overall had much smaller spread between PFTs than the other upscaled maps and sPlotOpen.

For P, the Butler and Vallicrosa maps showed larger differences between PFTs than sPlotOpen, while the Moreno map had a more similar level of differences (Fig. 4b). There was little similarity in the absolute values between sPlotOpen and the upscaled maps except for EBF which consistently had the lowest values for the upscaled maps and sPlotOpen. The difference between TWM and CWM was considerably smaller for P than for SLA and N.

We found considerable differences between upscaled maps regarding their agreement with sPlotOpen in terms of the within-PFT trait variation. Moreover, different maps showed the best agreement with sPlotOpen for any given trait and PFT with none of the maps clearly showing the overall best performance (Fig. S8). In particular, the Butler maps tended to perform well for forest PFTs, with the largest differences to other maps for ENF. However, the high values of the Butler SLA and P maps for SHR and DBF in the high latitudes disagreed with sPlotOpen that showed either a decrease (SLA) or no strong increase (P). Moreno tended to show better agreement with sPlotOpen for SHR and GRA, especially for SLA. Schiller, an Env approach, showed the strongest agreement to reference products for SHR and GRA for SLA, and overall robust performance for the other PFTs except ENF. There are indications that some of the Env maps show better agreement to the within-PFT variation of CWM than TWM, e.g. for the Boonman trait - PFT pairs of SLA - SHR and N - ENF (Fig. S8b).

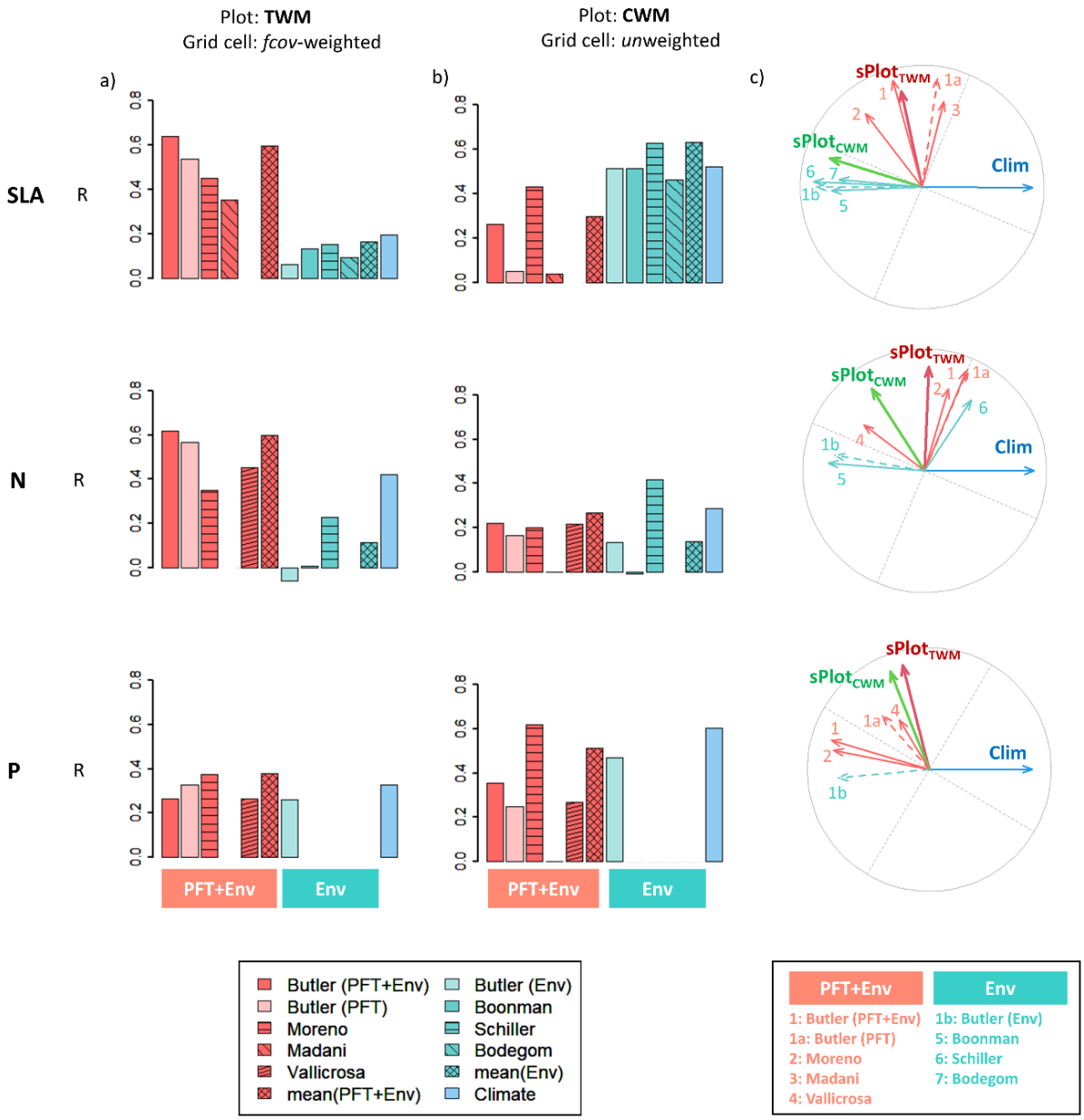

Figure 6: Comparison of upscaled maps against grid-level sPlotOpen data at 0.5°. The left column a) shows the correlation between upscaled maps against top-of-canopy weighted mean (TWM) sPlotOpen data scaled to the grid by weighting with the land cover fraction (fcov) corresponding to each plant functional type of the. The middle column b) shows the correlation between upscaled maps and community weighted mean (CWM) sPlotOpen data scaled to the grid without weighting. Colors refer to the grouping into maps that mostly only used environmental drivers (Env) or additionally used plant functional type and land cover information (PFT+Env). The blue colored bars indicate the highest correlation of sPlotOpen to a single environmental variable (among those used by Butler et al., 2017). The right column c) shows principal component biplots (first two axes) of upscaled maps, sPlotOpen data, and the climate variable (Clim) with the strongest relationships to Env maps (total annual solar radiation for SLA and N, mean annual temperature for P). In a) and b), the mean over the two upscaling groups excludes the different versions of Butler (only PFT, only Env) and the climate cases.

We found rather low grid-cell to grid-cell correlations of the upscaled maps vs. sPlotOpen at the level of individual PFTs/LCTs. Moderate to strong correlations only emerged when pooling data from all PFTs/LCTs (Fig. S10). In particular, the Butler maps showed high correlations with the difference to the Moreno map mostly being its lower SLA and N values for ENF. The improved Butler categorical maps showed a similar level of correlation as the PFT+Env map confirming that the correlation in the results with pooled data is strongly driven by between-PFT trait differences.

Without PFT stratification

Overall, we found that the upscaled maps showed moderate correlations (R up to 0.6) to sPlotOpen when matching the leaf-to-grid scaling of sPlotOpen to that of the upscaled maps (Fig. 6a for PFT+Env maps, Fig. 6b for Env maps). When comparing upscaled maps to sPlotOpen scaled to the grid cell with a different approach than was used in the upscaling approaches (Fig. 6b for PFT+Env maps, Fig. 6a for Env maps), the correlations to sPlotOpen were considerably lower for SLA and N (R = 0.2 - 0.4). For P, however, there were large differences between the scaling options for the PFT+Env maps but they did not follow the same pattern as for SLA and N except for the Butler Env map. In particular, the highest correlation of PFT+Env maps (Moreno) to sPlotOpen was to CWM without LCT cover weighting.

Even when only considering consistent leaf-to-grid scaling of sPlotOpen and the upscaled maps, there were notable differences between individual maps of the upscaling categories (Fig. 6). In the group of PFT+Env maps, the Butler map agreed best with sPlotOpen cover-weighted TWM and the (optimized) categorical map (PFT) showed similar performance as the full upscaled map. The Moreno map showed similar agreement to sPlotOpen cover-weighted TWM as Butler for SLA, but lower correlation for N and higher correlation for P (Fig. 6a). However, the Moreno map tended to agree better with sPlotOpen unweighted (at grid cell level) CWM, with considerable differences for SLA and P and similar correlation for N (Fig. 6b). Among the Env maps, the Schiller map showed consistently better agreement to sPlotOpen unweighted CWM data than the other maps, especially for N (Fig. 6b).

We found a tendency of stronger univariate trait-environment relationships for the unweighted CWM grid cell mean sPlotOpen trait values compared to the LCT cover weighted TWM (Fig. 6b, c). This was most pronounced for SLA and P where a single environmental predictor

showed similar levels of correlation to sPlotOpen data aggregated to grid cells without weighting as the 'best' upscaled Env maps.

Due to the complexity of the results, an overview of the key findings and the corresponding results figures is given in Table 3 that can be used alongside the detailed results description above.

Table 3: Overview of key results and the corresponding figures.

Key results	**Main figures**	**Supplementary figures**
Two fundamentally different categories of maps/upscaling approaches using mostly only environmental drivers (Env)‡ or additionally PFT† and land cover (PFT+Env)	Figs. 1, 2, 3, 4, 5, 6, 7	Figs. B1, S4-S9, S12-S14
PFT+Env maps strongly driven by PFT and land cover due to dominance of between-PFT over within-PFT trait variation; Env maps strongly driven by key environmental drivers	Figs. 3, 6, 7	Figs. S5, S12, S13
Larger between-PFT differences for PFT+Env than for Env maps; Overall PFT+Env more consistent with sPlot for between-PFT, similar performance for within-PFT trait variation	Figs. 4b, 5	Figs. S7, S8, S13
Wide, multi-modal trait distributions for PFT+Env maps and sPlot plot-level TWM* vs. narrower, unimodal distributions for Env maps and sPlot plot-level CWM§	Figs. 5, 8c	Figs. S11, S16a
Strong impact of leaf/plot-to-grid scaling on evaluation with sPlot data	Fig. 6a-c	Figs. S15
leaf-to-grid scaling: larger impacts of (horizontal) weighting with land cover fractions vs. no weighting dominates over vertical weighting (TWM/CWM)	Figs. 6c	Figs. S5c, S11, S12, S16b
Most sPlot data are located in heterogeneous grid cells; stratifying by PFT can considerably reduce the within-grid cell trait variability, especially for TWM	Fig. 8a,b	Fig. S15
Impacts of unweighted averaging of in-situ data to grid cells results in strong dependence of resulting trait distributions on grid cell size	Fig. 8c	Fig. S11

† PFT: plant functional type

‡ Env: environmental predictor variables (climate, soil)

* TWM: for top-of-canopy weighted mean

§ CWM: community weighted mean, and 'sPlot' refers to sPlotOpen

4. Discussion

We comprehensively compared seven approaches for the global upscaling of foliar trait data for SLA, and mass based leaf N and P concentrations. For each trait, we found considerable differences between the global maps (Fig. 2, Fig. A2) and identified two clearly separated groups of upscaling approaches (Figs. 2, 3): one using PFT and land cover information in

addition to environmental predictors and one mostly only relying on environmental predictors. Since the use of PFT information explained the main differences between the upscaled maps (despite various other methodological differences), it is important to address the question of what using PFT information versus not using it implies, and what the motivations behind these different approaches are. Also, while there is a close association of using top-of-canopy weight mean (TWM) together with PFT information in the existing upscaled maps, the choice of upscaling TWM or community-weighted mean (CWM) should be considered separately from the use of PFTs as these two aspects are not necessarily linked.

4.1 Upscaling with or without PFT and land cover information ?

Both the PFT+Env and the Env upscaling approaches have practical advantages and limitations which partly depend on the characteristics of the *in-situ* data (Table S5). We found that the Env-based maps do not capture the between-PFT trait differences (Fig. 4b) and tend to show stronger similarity to key environmental drivers (Figs. 6, 7c, Figs. S12b, S13), while they apparently reasonably capture environmentally driven within-PFT variations (Fig. S8). This is directly opposed to the categorical maps that only rely on PFT and LCT information to represent between-PFT differences while, by design, lacking information on within-PFT trait variation (Fig. 7c, Table S5). PFT+Env approaches can combine the two to capture both between- and within-PFT trait variation (Figs. 4b, 5, 7, S8). Clearly, the benefits of including PFT information depend on the level of between-PFT differences of the targeted trait, with SLA and N showing larger differences than P (Fig. 4b). Our results show that although including PFT and LCT information appears necessary to capture between-PFT trait differences in the upscaling approaches we examined, it is not sufficient to guarantee good performance (Figs. 4a, 5, Table S5). The motivations and limitations of global trait upscaling with and without PFT and land cover information are discussed in more detail below (4.1.1 - 4.1.3).

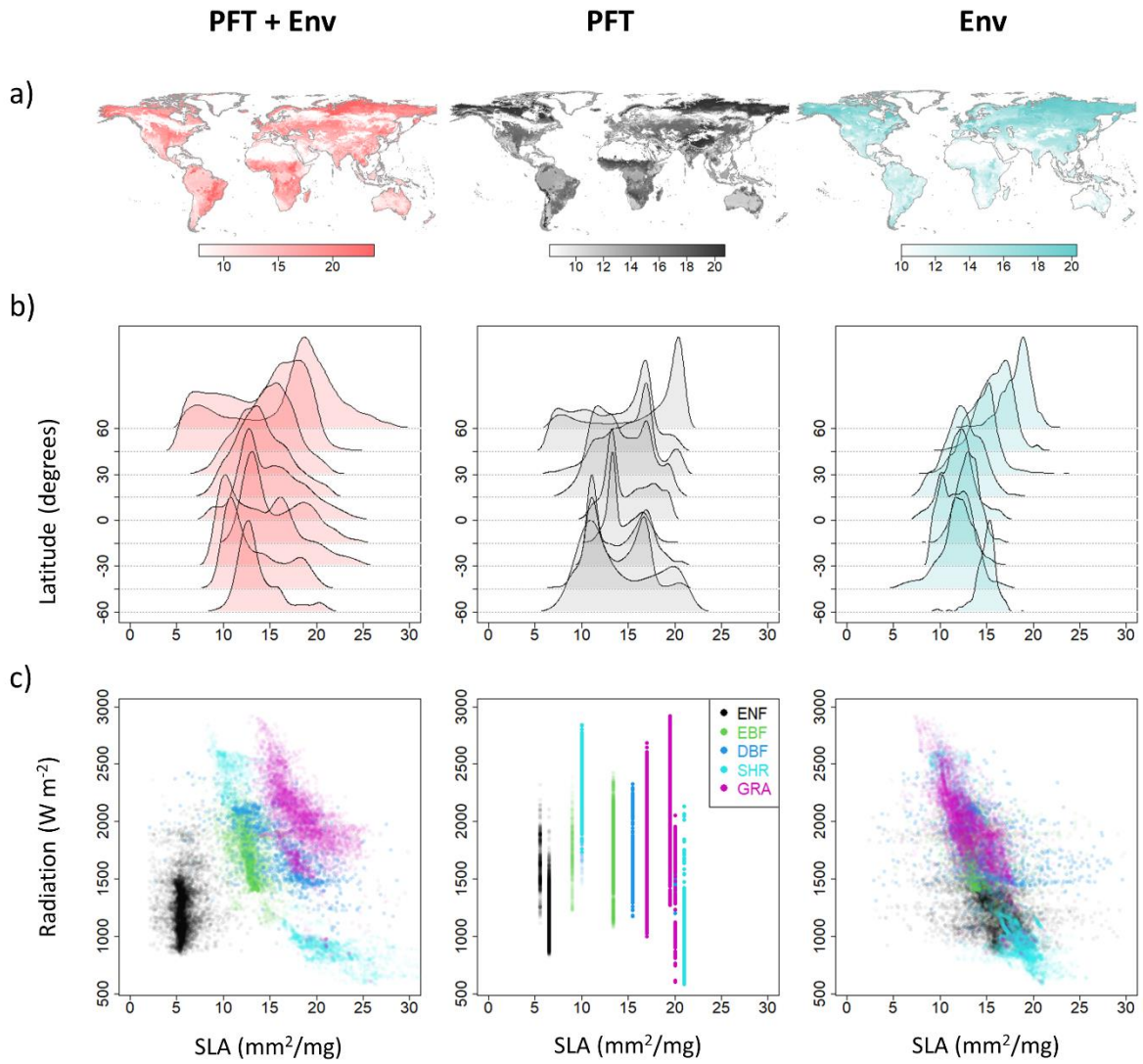

Figure 7: Overview of the impact of different upscaling approaches on maps, latitudinal trait distributions and the corresponding trait-environment relationships using consistent trait inputs and processing. a) maps of specific leaf area (SLA) for three different upscaling approaches applied to the same in-situ top-of-canopy weighted mean (TWM) data by Butler et al. (2017): the full upscaling model ('PFT+Env') using environmental predictors, plant functional type (PFT) and land cover information, the simplified categorical map ('PFT') only relying on land cover fractions and mean PFT trait values for 14 PFT categories, and the maps only relying on environmental predictors ('Env'). The color scales are optimized to maximize contrast for each map. b) the latitudinal distributions corresponding to the maps. c) the relationships between annual mean daily total solar radiation and the SLA values of the maps shown in a) stratified by land cover type (ENF: evergreen needleleaf forest; EBF: evergreen broadleaf forest; DBF: deciduous broadleaf forest; SHR: shrubland; GRA: grassland). For each land cover type only grid cells with more than 50% cover are shown. The categorical map ('PFT') in b) can have multiple trait values per land covre type as 14 PFT categories were used by Butler et al. (2017).

4.1.1 Upscaling with PFTs

We identified three different perspectives on using PFT and land cover information in upscaling approaches that are described in more detail below. Importantly, the PFT+Env upscaling approaches do not directly constrain trait values with PFT information in contrast to the categorical maps. Instead, the *in-situ* trait data, including its inter- and intraspecific components, determine the trait variation within each PFT and only the *spatial occurrence* of a given PFT is constrained by the land cover (LCT) products.

(1) **Refining the PFT representation in models.** To account for the variation of foliar traits within PFTs while keeping explicit PFT categories, the PFT+Env upscaling approach is a suitable choice. However, the PFT-based terrestrial biosphere models should not use the final traits maps including LCT weighting but would instead apply such weighting to the model outputs after using PFT-specific trait maps. Therefore, it is somewhat surprising that none of the PFT+Env maps provided separate maps per PFT although some of them were motivated by modelling applications (Fig. 1). An alternative strategy for better representing within-PFT trait variation without upscaling is to generate trait distributions per PFT instead of a single value (Butler et al., 2022).

(2) **PFT as a useful categorical predictor (spatialization).** As trait-environment relationships can differ between PFTs (Fyllas et al., 2020; e.g. Wright et al., 2005), including PFT information can considerably improve the predictive performance of trait-environment relationships (Kambach et al., 2023; e.g. Reich et al., 2007). Therefore, including PFT information appears attractive to improve regression models for the spatialization by building one Env submodel per PFT (Butler, Madani, Vallicrosa). PFT-related information for all grid cells is only needed for a final, global trait map that combines all PFTs. For this, the LCT maps are crucial to characterize the PFT cover within grid cells.

(3) **PFTs as tool to account for the lack of representativeness of *in-situ* observations.** *In-situ* trait observations were not designed to represent the large grid cells used in the upscaling but are collections from independent measurement campaigns for very different purposes (Kattge et al., 2020, 2011). More importantly, most of the *in-situ* observations used in the upscaling approaches fall into grid cells with heterogeneous land cover (Fig. 8a).

Therefore, the *in-situ* data in most grid cells are unlikely representative of the entire grid cell. To account for this lack of representativeness, two strategies can be applied. First, averaging traits per PFT within each grid cell and then weighting by PFT cover fraction using LCT cover products before applying the spatialization (Moreno). Such approaches have also been applied for scaling canopy structure-related trait observations to larger grid cells in heterogeneous landscapes (Hufkens et al., 2008; Shi et al., 2015). Second, separately upscaling per PFT before combining them in a final step using LCT data (Butler, Madani, Vallicrosa). This approach can both reduce within grid-cell trait variations and apply separate trait-environment relationships per PFT (see (2) above). The basis for both strategies is that the within-grid cell trait variability is considerably reduced when stratifying by PFT, reaching a reduction of about 50% for SLA TWMs (Fig. 8b) which is consistent across a wide range of spatial scales (Fig. S15). As this reduction corresponds to between-PFT trait differences (Fig. 4b), similar results are expected for N but a smaller reduction for P.

One important aspect of using PFT and LCT data in the upscaling is that, in contrast to unweighted averaging, it leads to results that are relatively insensitive of the grid cell size. This is based on two aspects. First, if fractional LCT cover is used, the relevant sub-grid information is accounted for and this leads to a strict independence of resolution in case of categorical maps. Second, the trait distributions of PFTs do not show a strong dependence on grid cell size and the between-PFT trait differences are maintained even at very coarse resolutions (Fig. 8c) which implies the benefits in the leaf-to-grid scaling and spatialization apply across resolutions. While nonlinearities in the trait-environment relationships could lead to some impacts of grid cell size, the fact that we found the strongest agreement between the Butler and Moreno maps (Fig. 4) that used 50 km and 1 km grid cell sizes for upscaling, respectively, indicates these impacts are likely small compared to other factors.

While PFT and LCT information can be very useful for trait upscaling, there are limitations both with respect to PFT and LCT concepts and data products.

Limitations of using in-situ PFT data. The definition of (dominant) PFTs we used is based on growth form, leaf type and leaf phenology. This choice is useful in practice as the categories align well with the first two axes of the global spectrum of plant form and function (Díaz et al.,

2016) and can be reasonably well mapped from remote sensing. However, it is necessarily a simplification and not an optimal decomposition of trait distributions into parts that minimize overlap. Another limitation is that some species can change PFT categories depending on the environmental conditions (H. Wang et al., 2022), but this likely affects a relatively small fraction of species. While some of these limitations could be partly addressed/reduced with finer PFT categories by adding climatic information (as done by Butler and some terrestrial biosphere models) this appears unnecessary if environmental drivers are used to model within PFT trait variation with sufficiently complex models.

Limitations of using LCTs. First, by definition, the LCT categories only have a minimum cover threshold (Loveland and Belward, 1997) and do not quantify the *actual* canopy cover which would be needed. This can have an impact on the meaning of TWM in practice and change it towards the weighted mean of the dominant rather than the taller PFTs. Second, the maps of LCT cover can have considerable uncertainties even when considering only the original land cover class definitions (Congalton et al., 2014). Given these uncertainties and dominant impacts of the land cover information at both the global and more local scales (e.g. Figs. S4, Fig. S5), the differences between the PFT+Env maps could therefore be partly explained by discrepancies between the land cover products used by the different upscaling approaches (Table S2). Third, since the LCT cover is not available for future time periods, or only with even larger uncertainties than the corresponding climate scenarios, using LCTs in upscaling is more suitable for diagnostic purposes, i.e., monitoring, than for predictive purposes.

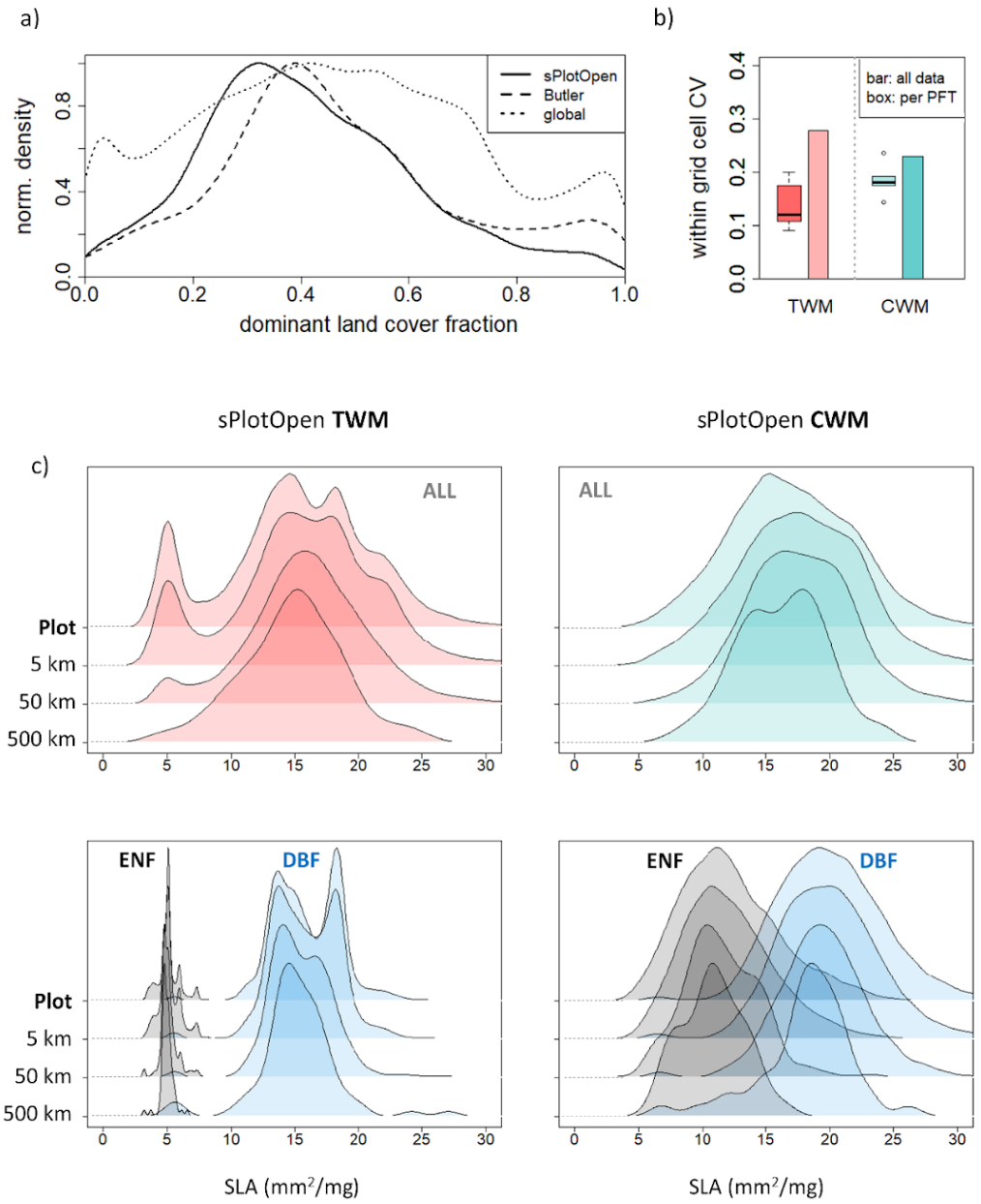

Figure 8: Overview of the impact of different upscaling approaches on latitudinal trait distributions and key aspects related to the heterogeneity of the vegetated land surface. a) distribution of grid cells regarding the maximum land cover fraction irrespective of the land cover type: sPlotOpen (all plots, N~5000), TRY data selected by Butler et al. (2017)(N~500), or all global vegetated grid cells (N~60000). The maximum fraction represents a measure of land cover homogeneity. b) sPlotOpen global-scale within grid cell (50 km) trait variability as quantified by the coefficient of variation (CV) based on top-of-canopy weighted mean (TWM) or community weighted mean (CWM) data and all available trait data (bar showing median over the global-scale distribution) or stratified per PFT (boxplot summarizing the global medians of the individual plant functional types, i.e., PFTs). c) example of the impacts of unweighted averaging on sPlotOpen TWM and CWM trait distributions in the latitudinal range of 45°-60° north either including all data ('All' in top row) or stratified by PFT for evergreen needleleaf forest (ENF) and deciduous broadleaf forest (DBF). Plot data are shown for

reference and three different grid cell sizes with their corresponding size at the equator are given. Conceptually, in c) the top panels correspond to the bars in b), while the bottom panels correspond to the boxplots in b).

4.1.2 Upscaling without PFTs

Due to the limitations of PFT categories and LCT products, upscaling without them seems preferable conceptually. Especially if the focus is on upscaling CWMs, relying on PFT information can seem unattractive as differences between dominant PFTs are smaller than for TWMs (Fig. 4b, 8b). Third, assuming that the environmental predictors are available for future scenarios with a reasonable level of confidence, Env approaches could then be used for estimating future changes in foliar traits (e.g. Boonman et al., 2022).

Upscaling approaches that do not rely on PFT information, however, face important practical limitations. These limitations affect both the leaf-to-grid and spatialization steps, but the impacts on the leaf-to-grid scaling are considerably more important as information lost in this step cannot be recovered in the spatialization. The limitations affect upscaling of TWM more strongly than CWM but are relevant in both cases.

Limitations in leaf-to-grid scaling. In the leaf-to-grid scaling, the unweighted averaging over available *in-situ* data effectively assumes either that these data are representative of the grid cells or that there might be biases at smaller scales that average out when looking at global scale trait patterns. These assumptions are addressed separately below.

The assumption of representativeness is not well justified for the following reasons. First, none of the relevant *in-situ* data sources like TRY, sPlotOpen, or citizen science images (Schiller) were sampled in a manner to provide trait information that representatively capture variations within 0.5° grid cells, i.e. heterogeneous grid cells are not well characterized by in-situ trait data. Second, the large majority of grid cells that have in-situ trait data from TRY (used by Butler) are heterogeneous in terms of LCTs (Fig. 8a) and given the trait differences between PFTs (Fig. 4b) also in terms of foliar trait variation. Due to a large fraction of the global vegetated land surface being heterogeneous regarding LCT cover at 0.5° (Fig. 8a), larger numbers of globally distributed in-situ data do not result in higher fractions of grid cells with data that are homogeneous if they are not designed specifically with this goal. This can be seen when comparing the TRY data used by Butler with sPlotOpen data used for evaluation that covers about a factor 10 more 0.5° grid cells but even shows a tendency towards higher levels

of LCT heterogeneity (Fig. 8a). Therefore, the even larger number of grid cells covered by citizen science data used by Schiller and Wolf et al. (2022) or the most recent version of TRY with considerably more data is also expected to show comparable levels of LCT heterogeneity as the global land surface. In this context, it is worth mentioning that the high levels of heterogeneity is not restricted to the coarse 0.5° grid cells but also shows high levels for the 1 km grid cells (Yu et al., 2018) used by Moreno and Vallicrosa (Table 2).

The impact of the lack of representativeness of *in-situ* observations is not limited to small spatial scales. While the impacts can differ between traits and across the global land surface, they are most conspicuous when looking at the low values of SLA and N for ENF. The original *plot-level* sPlotOpen TWM (and *in-situ* TRY) data show a distinct double-peak distribution for SLA in the higher northern latitudes. However, the peak feature with lower SLA values associated with ENF is either strongly reduced or almost disappears when applying unweighted averaging the *in-situ* data within grid cells and these impact strongly depend on the grid cell size (Fig. 8c, Fig. S11). Due to the loss of information already for the reference or training grid cells, the lower trait signal of ENF cannot be well modeled in the spatialization resulting in the absence of a distinct signature of lower SLA and N values in the ENF-dominated region of the northern hemisphere of the Env maps (Figs. 3, 4). This effect of suppression of the low trait values for ENF in upscaled maps without PFT information can also be seen in the Env versions of the Butler and Moreno upscaled maps (Figs. S5, S12a) demonstrating that this effect is not related to the selection of *in-situ* data.

The limitations regarding unweighted leaf-to-grid scaling do not only apply to upscaling approaches that applied the leaf-to-grid scaling as first step (Boonman, Bodegom) but also to approaches that first spatialize and then scale a considerably larger number of trait estimates to the grid cells (Schiller) (Fig. 1). The reason for this is that a larger number of grid cells without targeted sampling towards more homogeneous grid cells does not noticeably change the level of heterogeneity (Fig. 8a). In this context, the approach by Wolf et al. (2022) that is conceptually similar to the Schiller approach regarding the first step of the upscaling (Fig. 1) is also worth mentioning. The maps of Wolf et al. (2022) used species information rather than RGB images from citizen science and are most strongly correlated to the Schiller maps (results not shown) and consequently would be grouped together with Env maps in a PCA analysis (Fig. 2) even though no environmental predictors were used. In fact, the spatial patterns of the Schiller map are also mostly determined by the the RGB images and the Env predictors mostly

led to smoother patterns (Schiller et al., 2021). Thus, the larger similarity of the Schiller and Wolf et al. (2022) maps with the maps that only used environmental predictors is due to the leaf-to-grid scaling not the spatialization. In this sense, the Env group in Fig. 2a actually represents the group of maps that did not use PFT information rather than the group that only used environmental predictors.

Limitations in the spatialization. In principle, only using environmental information in the spatialization implies using universal trait-environment relationships across all vegetation types (Figs. 7c, S13), which results in limitations to capture trait differences between PFTs (Kambach et al., 2023; e.g. Reich et al., 2007). This limitation could be overcome by using additional predictors that contain information on PFTs/LCTs. However, we found that without also accounting for between-PFT differences in the leaf-to-grid scaling, adding such predictors results in similar limitations regarding between-LCT differences as not using such additional predictors. In case of the Schiller approach, the RGB images used in the spatialization contain information on PFTs/LCTs but the maps show inconsistent between-LCT differences compared to sPlotOpen (Fig. 6b). Moreno combined Env predictors with with satellite reflectance time series (that contain information on PFTs/LCTs) in the spatialization and we found that the PFT information in the leaf-to-grid scaling was necessary to capture the patterns of between-PFT differences effectively (Figs. S5a,b, S12a). Somewhat related to this, only using environmental predictors likely increases the uncertainties of spatialization in regions with low in-situ data density. Maps using PFT information effectively have (implicit) additional constraints from LCT predictors in locations without in-situ data as the variation within some LCTs, e.g. ENF, is much smaller than the trait ranges for all LCTs combined. Consistent with this interpretation and in contrast to the PFT+Env maps, the differences between Env maps (Fig. 3) seem to be at least partly related to *in-situ* data availability (Fig. S1). Also, it is noteworthy that the Env maps that partly captured somewhat lower values for ENF only did so in smaller parts of the ENF-dominated regions (e.g. Boonman for N, Fig. B1) such as Europe that has a relatively high density of *in-situ* observations (Fig. S1). At least for the Boonman map, the failure to capture the low ENF trait values in North America and Siberia also appears to be related to extrapolation in the environmental predictor space (Boonman et al., 2020) in addition to the aggregation effects due to heterogeneous grid cells in the leaf-to-grid scaling (Figs. 8c, S11).

Another relevant aspect is that only using environmental predictors results in patterns that better represent *potential* vegetation that could grow in a certain place given the

environmental conditions rather than the vegetation that is *actually* growing there. Using remote sensing predictors can partly compensate for this as direct information on surface characteristics is included (Fig. S7a). This perspective of potential vs. actual vegetation regarding the use of environmental and remote sensing predictors has also recently been described in the context of species distribution modelling (Bonannella et al., 2022).

4.1.3 Limitations affecting both approaches with and without PFT information

While the different limitations appear to clearly separate the approaches with and without PFTs at first sight, there actually is some overlap between them due to the characteristics of the underlying *in-situ* data. The key limitation of *in-situ* data is that it is mostly located in heterogeneous grid cells regarding land cover (Fig. 8a). This implies that even when weighted averages using LCT cover fractions are used in the leaf to grid scaling step (Moreno approach), the result is a combination of trait values from different LCTs, which has a rather similar impact on latitudinal trait distributions as unweighted averages, i.e. making the distributions narrower and more unimodal (Fig. S16a). Based on this, the Moreno approach (PFT+Env) that only used PFT+LCT information in the leaf-to-grid scaling and Env in the spatialization (Figs. S5a, S12a,c) tends to effectively generate trait estimates that better represent heterogeneous grid cells. This results in considerable discrepancies between upscaled maps and the plot-level *in-situ* data for more homogeneous grid cells, which account for an important part of the global vegetated land surface despite the dominance of heterogeneous grid cells (Fig. 8a). While the final model by Moreno used remotely sensed surface reflectance time series, which have a similar information content as the LCT cover products, in the spatialization, this model could apparently not fully recover the trait values of homogeneous grid cells (Figs. 4b, 6, S8a).

Both the PFT+Env and the Env approaches apparently face challenges to capture the trait values of deciduous needleleaf forest (DNF). The PFT+Env approaches that separately upscaled per PFT such as Butler, Madani and Vallicrosa simply lack enough *in-situ* data to well constrain DNF-specific models. The Env approaches face the challenge that available *in-situ* data in locations not dominated by DNF are not representative of the environment where DNF is dominant (Boonman et al., 2020). Recent advances in optimality theory-based trait modeling could help to better constrain the trait values of SLA and N for DNF-dominated regions despite the current lack of *in-situ* observations (Dong et al., 2023).

4.2 Vertical variation of traits within the canopy: upscaling CWMs or TWMs ?

Apart from the horizontal scaling aspects related to the use of PFTs and land cover, the differences in the upscaling approaches regarding the way vertical trait variation was accounted for (CWMs versus TWMs) is an important aspect to consider. Note that the 'vertical' here only refers to the different vegetation layers as impacts of vertical within-canopy gradients on traits were not considered by upscaling methods given that the input trait values in the large databases are typically from sunlit leaves. While the use of CWMs versus TWMs has considerably smaller impacts on spatial trait patterns than upscaling with PFTs and LCTs or not (Figs. 6c, S5c, S16), it is an important additional factor resulting in differences between maps. Similar to unweighted averaging in the leaf-to-grid scaling (Fig. 8c), using CWMs tends to result in narrower and more unimodal trait distributions with smaller differences between PFTs than for TWMs (Figs. 4b, 6, 8, S7). However, the differences between TWM and CWM depend on the trait. Among foliar traits, we found larger differences for SLA than for N and P (Fig. S16b), which is consistent with the known sensitivity of SLA to light availability (Evans and Poorter, 2001) and other evidence on vertical variation (Davrinche et al., 2023; Ellsworth and Reich, 1993).

Conceptually, CWM and TWM correspond to an intermediate step in the leaf-to-grid scaling. In the case plot data such as sPlotOpen, CWM and TWM are approaches to scale leaf-level trait observations to the plot or community level. Then, there is a final step of scaling from plots or communities to the grid cell level. While this separation of leaf-to-grid scaling intwo two steps is straightforward for sPlotOpen data, it is more challenging to apply with TRY data although Boonman did this by sub-selecting datasets that represent plant communities.

While none of the upscaling approaches used CWM or TWM in the same way as done in sPlotOpen, there are nevertheless tendencies towards one or the other. A more detailed discussion on the motivations and limitations of CWMs and TWMs follows below.

4.2.1 CWMs

CWMs are the standard metric for many ecological analyses based on community trait data including trait-trait and trait-environment relationships (Anderegg, 2022; Bruelheide et al., 2018; Guerin et al., 2022), and are routinely applied in the sPlot and sPlotOpen datasets (Bruelheide et al., 2019; Sabatini et al., 2021). The concept of CWMs was introduced in relation to the biomass ratio hypothesis, which states that species contribute to ecosystem

characteristics based on their biomass ratio (Garnier et al., 2004), as should their traits. The weighting of traits is commonly done by the basal area, biomass, or leaf area (Anderegg, 2022) or by fractional cover (Sabatini et al., 2021). The goal of CWMs is to integrate all trait variation present in a plant community in a single value that is expected to show more consistent trait-environment relationships than sub-selections of the community (Anderegg, 2022). Among the upscaling approaches, Boonman used unweighted community means and the Schiller approach likely implicitly considers trait variation from different parts of the canopy visible in the RGB images used in the trait prediction.

4.2.2 TWMs

Upscaling top-of-canopy-weighted means (TWMs) can have several different motivations related to terrestrial biosphere modeling, alternatives to the common cover/abundance-based weighting in CWMs, and remote sensing. From the perspective of terrestrial biosphere modeling, the higher levels of a canopy tend to dominate many processes of vegetation-atmosphere interactions such as photosynthesis due to the dominance of leaf area and light availability of top-of-canopy vegetation (Musavi et al., 2015). Therefore, the trait values of sunlit leaves of dominant PFTs have been widely used in land surface models (Yang et al., 2015). Impacts of reduced light availability that can capture part of the trait variation in lower levels of a canopy are commonly modeled in land surface models (Hikosaka et al., 2016), therefore, the combination of such models with TWM trait values can be useful.

Even when ultimately aiming at CWMs, TWMs can be a relevant practical tool to approximate other weighting strategies when only relative cover fractions are available as is the case for sPlotOpen (Sabatini et al., 2021). In fact, TWMs can be interpreted as pragmatic proxy for biomass-weighted CWMs assuming that the (leaf) biomass of understory vegetation can be neglected compared to the dominant overstory contributions. In contrast, CWMs using relative cover give similar weight to understory vegetation as overstory trees as long as their cover fractions are comparable irrespective of large differences in leaf area and biomass. The PFT-based upscaling approaches (Table 2) effectively all used unweighted top-of-canopy means as they averaged all relevant in-situ trait data corresponding to a given PFT.

From a practical remote sensing perspective, sensors on air- and spaceborne platforms are most sensitive to the top of the canopy. Therefore, if the goal is to compare upscaled maps with remote sensing-based maps, TWMs are a suitable metric. This can also be illustrated with plant

height for which there are already global maps derived from satellite-based lidar instruments (Lang et al., 2022; Potapov et al., 2021; Simard et al., 2011; Wang et al., 2016). While plant height is admittedly an extreme case due its large differences between CWM and TWM, it can serve as an intuitive example to illustrate the differences in these two metrics: clearly, TWM, which corresponds to canopy (top) height is expected to be much larger than CWM plant height that includes understory vegetation. Unsurprisingly, upscaled plant height maps based on TWM show a considerably higher level of similarity to satellite-based canopy height maps using lidar information than CWM upscaled maps (Fig. S14). Importantly, the TWM and CWM upscaled maps differ not only considerably regarding their absolute values but also show large differences in their spatial patterns (Fig. S14). In addition to the difference of using TWM or CWM, the height maps also differed in the use of PFT/LCT data (only used for TWM). In contrast to foliar traits, however, for canopy height impact of using PFT information is considerably smaller than the choice of TWM versus CWM, in contrast to the foliar traits (Fig. S16b).

4.3 Evaluation of maps

While the comparison of different upscaling approaches and maps can give important insights into the factors explaining the differences, a higher level of consistency - as observed in the maps using PFT information (Fig. 2) - does not necessarily imply better performance. Therefore, it is important to take other criteria into account.

4.3.1 Internal performance metrics.

Most of the upscaling approaches provided cross-validation metrics, but their interpretation is complex. Overall, there was a clear pattern of considerably higher R^2 for PFT+Env approaches compared to Env approaches (R2 about 0.6 or higher for PFT+Env compared to 0.4 or lower for Env), with larger differences for N compared to SLA. However, these findings can be misleading as the input *in-situ* trait observations differ considerably in terms of the number and the data sources (Fig. 1) and there are limitations of random cross-validation approaches to evaluate mapping performance (Meyer and Pebesma, 2021; Ploton et al., 2020).

Some of the upscaling products also provided estimates of the uncertainty of the mean (standard error) trait values per grid cell. However, these estimates differ considerably in terms of methodology and should be interpreted with caution. Overall, we found no indications that

the uncertainty or variability estimates corresponded to the observed discrepancies between maps, even within the PFT+Env and the Env groups (Figs. 4, S17).

4.3.2 External reference data (sPlotOpen)

Despite its limitations, we think that sPlotOpen is currently the best available open access dataset for evaluating the upscaled maps given its global coverage and the fact that it is based on a characterization of entire plant communities in contrast to individual species. However, as the upscaling approaches differ in the way horizontal (within-grid-cell) and vertical (within canopy) trait variation was taken into account, there is no way to process sPlotOpen data such that it could be used as universal benchmark at the *grid cell* level for all upscaling approaches. Rather, sPlotOpen can be used as a basis for evaluating the differences in performance *within* a given upscaling framework/strategy regarding the leaf-to-grid scaling. When comparing *plot-level* sPlotOpen data to upscaled maps (Figs. 2a, 6, S9), the upscaling approach-specific adjustment to sPlotOpen data can be restricted to the choice of plot-level trait metric (CWMs or TWMs).

We found that grid-cell-level trait distributions are strongly impacted by trait heterogeneity, with a tendency towards a narrowing of distributions (Fig. 8a,b). Importantly, the trait distributions of *unweighted* averages strongly depend on the chosen grid cell size (Figs. 8b, S11), with smaller grid cell sizes showing trait distributions more similar to plot-level data. These impacts are primarily due to the unweighted averaging as the trait distributions stratified per PFT showed a high level of stability across a wide range of grid cell sizes (Fig. 8b).

Regarding the evaluation of PFT+Env maps with grid-cell-level sPlotOpen data, our results indicate that a comparison stratified per PFT (Figs. S7, S8) is more meaningful than at the level of the final maps. First, when using the final maps after applying the LCT cover-weighted averages, highly simplified categorical trait maps, which were the motivation for improvement using PFT+Env upscaling, can achieve a similar level of agreement with sPlotOpen reference data (Fig. 6a). Second, the PFT-stratified evaluation directly quantifies the similarities between upscaled maps and sPlotOpen at the level of within-PFT trait variation that was the main motivation of the upscaling (e.g. Butler). To facilitate such evaluations at the level of individual PFTs, future upscaling products should be provided both as final global trait maps and its underlying PFT component maps. While we showed that the final maps can, in principle, be separated into PFT components (Appendix A), this approach introduces unnecessary additional

uncertainties which can be avoided by using the direct outputs from the upscaling. Our findings also indicate that the between-PFT trait differences should be evaluated in addition to the within-PFT variations as, in contrast to what might be expected, they can differ considerably even between PFT+Env approaches (Figs. 4b, S8).

One limitation of the sPlotOpen dataset is that it ignores intra-specific trait variations as global-scale species mean trait values from the TRY database were used (Sabatini et al., 2021). The assumption of dominance of species composition and abundances on CWMs and TWMs might be justified for most regions. However, we found indications that the strong tendency of high trait values at high latitudes of the Butler maps was at least partly caused by strong intraspecific variations in the underlying *in-situ* data (Fig. S18). Therefore, it remains unclear to what degree the discrepancies between sPlotOpen and the Butler maps in high latitudes (Fig. S8) are due to limitations of the Butler maps or sPlotOpen-based trait estimates.

4.4 Synthesis maps

A relevant question for applications is whether generating synthesis maps per upscaling group (PFT+Env, Env) that outperform the individual maps is feasible and defendable. While the simple average over all maps for a given trait and upscaling category is useful for illustrating some general differences between the two upscaling category (Figs. 4-6), we did not find any evidence that these average maps performed better than the best individual map when evaluated with sPlotOpen (Fig. 6).

The simple approach of averaging maps to obtain a synthesis map has limitations. First, a weighted average with weights determined by performance to a benchmark would be preferable. Furthermore, given our findings that different PFT+Env maps performed best for different PFTs and that differences between the maps can be due to difference in LCT products, the preferred strategy for generating PFT+Env synthesis maps would be at the level of trait maps per PFT. Then, if needed, the synthesis maps per PFT could be converted to global trait maps by applying LCT cover weighting using a selected product. Due to the limitations of the separation of upscaled maps into their underlying PFT components, we could not apply this approach

4.5 Trait ratios, trait-trait, and trait-environment relationships

While our focus was on the comparison and evaluation of individual foliar traits other aspects of the upscaled maps such as trait ratios, trait-trait and trait-environment relationships are also relevant for ecological applications and could be seen as additional aspects to consider.

Trait ratios. In addition to SLA, and N and P, trait ratios such as N:P are also of interest for some applications. While it is straightforward to calculate trait ratios, such as N:P, from the individually upscaled traits, trait ratios should be directly upscaled for optimal results (Vallicrosa et al., 2022). For N:P this has only been done in relatively few approaches (e.g. Moreno-Martínez et al., 2018; Vallicrosa et al., 2022; Wolf et al., 2022).

Trait-trait correlations. Given the differences in individual trait maps, it is not surprising to also find large differences in trait-trait correlations, even within a given upscaling category (i.e. PFT+Env or Env). We indeed found considerable differences in trait-trait relationships both at the global scale and the local scales using the moving window approach (results not shown). An important aspect is that the trait-trait correlations of upscaled maps should not be expected to have the same characteristics as in-situ data. The reason is that for the PFT+Env maps that are strongly driven by patterns of LCT and mean PFT traits (Figs. 3, 4a, 8a), the trait-trait correlations are dominated by correlations at the level of mean PFT traits.

Trait-environment relationships. Given the differences between upscaled maps it is to be expected that the underlying trait-environment relationships also differ. We did this with the PFT stratified maps and sPlotOpen data, which reveals large differences both between the two upscaling categories and within them (Figs. 7c, S13). Similar to trait-trait relationships, trait-environment relationships should best be analyzed per PFT for the PFT+Env maps.

4.6 Future opportunities

Future upscaling efforts will benefit from progress in areas relevant for foliar trait upscaling related to both the leaf-to-grid and spatialization steps (Fig. 1). *In-situ* trait databases such as TRY have already been increasing in the volume of available data (Kattge et al., 2020) and the combination of different trait databases can further maximize the available data as shown by Vallicrosa. Furthermore, plot databases such as sPlot are also rapidly growing (https://www.idiv.de/de/sdiv/working-groups/wg-pool/splot/splot-database.html) and can also

be used as the basis for upscaling. However, increases in the amount of *in-situ* data do not necessarily lead to increased representativeness for grid cells (Fig. 8a). Regarding the evaluation, sPlotOpen data could potentially be refined to at least partly include intraspecific trait variation for species where sufficient data is available.

To reduce the uncertainties stemming from the leaf-to-grid scaling step in the upscaling, a logical approach is to decrease the size of grid cells to better match the resolution of the *in-situ* observations and increase the fraction of homogeneous reference grid cells. While some of the upscaling approaches used 1 km rather than the coarse 50 km grid cells (Table 1), the level of land cover heterogeneity at 1 km resolution is still high (Yu et al., 2018). Promising efforts make use of high-resolution air- and spaceborne imagery to directly link tree canopies to satellite remote sensing predictors and generate regional or national-scale trait maps (Aguirre-Gutiérrez et al., 2021; Asner et al., 2016), but have not yet been applied at the global scale.

Given the increase in the availability of satellite imagery with both high spatial and temporal resolution (e.g. Houborg and McCabe, 2018), there is potential to improve LCT cover maps to better approximate actual PFT cover fractions. Several improved products have already been generated (Harper et al., 2023; Macander et al., 2022; L. Wang et al., 2022). Harper et al. (2022) used high-resolution (30 m) tree cover and canopy height maps to refine global, long-term land cover products in an attempt to better approximate actual PFT canopy cover. Wang et al. (2022) applied a somewhat similar approach using only tree cover to Canada and Alaska. Macander et al. (2022) generated long-term, high resolution (30 m) top cover for seven PFTs across Alaska and parts of Canada. Also, individual tree crowns can now be detected at large scales (e.g. Mugabowindekwe et al., 2022; Wang et al., 2023) and could be further classified into PFTs with time series data or combined with existing high-resolution land cover products in approaches similar to Harper et al. (2022). All these efforts could help reduce uncertainties in upscaled maps that use PFT information.

Different approaches have been developed that try to use stronger predictors of foliar traits than environmental drivers and PFT information. On the one hand, *species occurrence* data from large databases such as GBIF or iNaturalist have been combined with machine learning techniques (Wolf et al., 2022) (Moreno-Martínez et al., in prep.) in an effort to make use of the strong predictive power of species and phylogeny (Kattge et al., 2011; Maynard et al., 2022; Vallicrosa et al., 2021). On the other hand, hyperspectral reflectance of plant canopies in the

visible and near-infrared range has already been successfully used to map some foliar traits at regional scales based on airborne remote sensing (Asner and Martin, 2016; Wang et al., 2020). Importantly, these applications demonstrated the ability to capture spatial, intra- and inter-annual temporal (Chlus and Townsend, 2022) and vertical trait variation (Chlus et al., 2020). Therefore, the hyperspectral-based trait mapping approach has great potential for operational, global-scale monitoring for some traits (Jetz et al., 2016), especially given that hyperspectral satellite imagery is increasingly becoming available (Zeng et al., 2022).

5. Conclusions and recommendations

We identified two categories of upscaling approaches that result in global, upscaled maps with strongly differing, and partly even opposed spatial patterns. Despite differences in many aspects of the upscaling approaches across these two categories, the use of PFT and land cover information was the dominant factor explaining the differences between the resulting maps. Differences in accounting for vertical trait variation (top-of-canopy versus community mean) were also relevant but had smaller impacts on the spatial patterns of foliar traits than the use of PFT and land cover data. Maps that used PFT and land cover information showed larger trait differences between PFTs and agreed better with sPlotOpen data than the maps mostly relying only on environmental predictor information. Not accounting for within-grid-cell trait variation tends to suppress extremes of the trait distributions, which effectively reduces trait differences between PFTs and leads to more unimodal trait distributions with larger impacts on top-of-canopy trait values. Importantly, these effects also show a strong dependence on grid cell size with stronger impacts at larger grid cell sizes. While the use of PFT and land cover information can partly counteract these effects, the land cover information introduces other uncertainties and has dominant impacts on the global spatial patterns of trait variation.

Based on the insights from our study, we identified four recommendations that are relevant for future upscaling and/or evaluation efforts:

1. Upscaling products should clearly specify the type of trait provided, which is determined by the metric used at the site or plot level (e.g. top-of-canopy versus community; weighted versus unweighted means; type of weighting factor), the type of scaling to the grid cell level (weighted/unweighted, type of weighting factor) and the type of predictor information used (i.e. environmental drivers, remote sensing data, land

cover products etc.). Upscaling products based on PFT information should provide the original maps for each PFT separately in addition to the overall product.

2. In the evaluation of maps with reference data such as sPlotOpen, comparable scaling as for the upscaled maps need to be applied to the reference data if the grid cell size is much coarser than the plot size (for grid-cell-level evaluation). Furthermore, comparisons of the distributions of *plot*-level reference data with those of upscaled maps can provide valuable additional insights. For maps using PFT and land cover information, an evaluation at the level of separately upscaled maps per PFT is recommended to directly quantify the agreement of between- and within-PFT trait variation independently of the impacts of land cover that dominate the final maps per trait.
3. Future upscaling efforts should aim at reducing uncertainties by better matching the scale of *in-situ* observations with high-resolution predictor data and ideally also by using predictors with a stronger link to foliar traits than environmental variables.
4. Future trait sampling efforts should consider the aspect of within grid cells trait variation in terms of land cover as well as representativeness at the global scale regarding geographic aspects and covering the full range of key environmental drivers.

Data and Code availability:

Most underlying data of global foliar trait maps are already publicly available (see links given in Table S3). Other maps can be requested from the first authors (Table 1). The code for the calculation of sPlotOpen TWM data is available online (https://github.com/fmsabatini/sTraits_GlobalIntercomparison). Other code used relied on existing functions of R packages that are specified in the methods section.

Acknowledgements

This paper is a joint effort of the working group sTRAITS kindly supported by sDiv, the Synthesis Centre of the German Centre for Integrative Biodiversity Research (iDiv) Halle-Jena-Leipzig, funded by the German Research Foundation (FZT 118, 02548816). Support for P.T., J.C.-B. and E.B. was provided by the NSF Biology Integration Institute ASCEND (DBI 2021898), with additional support for P.T. provided by NSF Macrosystems Biology and NEON-Enabled Science (MSB-NES) award DEB 1638720. A portion of this research was carried out at the Jet Propulsion Laboratory, California Institute of Technology, under a contract with the National Aeronautics and Space Administration (80NM0018D0004). This research was also supported by the European Research Council under the ERC-SyG-2019

USMILE project (grant agreement 855187). T.K. acknowledges funding from DFG for the project PANOPS (grant-no: 504978936). J.A.-G. was funded by the Natural Environment Research Council (NERC; NE/T011084/1) and the Oxford University John Fell Fund (10667). I.H.M.-S. was funded by the NERC grants ShrubTundra (NE/M016323/1) and Tundra Time (NE/W006448/1).

References

Aguirre-Gutiérrez, J., Rifai, S., Shenkin, A., Oliveras, I., Bentley, L.P., Svátek, M., Girardin, C.A.J., Both, S., Riutta, T., Berenguer, E., Kissling, W.D., Bauman, D., Raab, N., Moore, S., Farfan-Rios, W., Figueiredo, A.E.S., Reis, S.M., Ndong, J.E., Ondo, F.E., N'ssi Bengone, N., Mihindou, V., Moraes de Seixas, M.M., Adu-Bredu, S., Abernethy, K., Asner, G.P., Barlow, J., Burslem, D.F.R.P., Coomes, D.A., Cernusak, L.A., Dargie, G.C., Enquist, B.J., Ewers, R.M., Ferreira, J., Jeffery, K.J., Joly, C.A., Lewis, S.L., Marimon-Junior, B.H., Martin, R.E., Morandi, P.S., Phillips, O.L., Quesada, C.A., Salinas, N., Schwantes Marimon, B., Silman, M., Teh, Y.A., White, L.J.T., Malhi, Y., 2021. Pantropical modelling of canopy functional traits using Sentinel-2 remote sensing data. Remote Sens. Environ. 252, 112122. https://doi.org/10.1016/j.rse.2020.112122

Anderegg, L.D.L., 2022. Why can't we predict traits from the environment? New Phytol. nph.18586. https://doi.org/10.1111/nph.18586

Asner, G.P., Knapp, D.E., Anderson, C.B., Martin, R.E., Vaughn, N., 2016. Large-scale climatic and geophysical controls on the leaf economics spectrum. Proc. Natl. Acad. Sci. 201604863.

Asner, G.P., Martin, R.E., 2016. Spectranomics: Emerging science and conservation opportunities at the interface of biodiversity and remote sensing. Glob. Ecol. Conserv. 8, 212–219. https://doi.org/10.1016/j.gecco.2016.09.010

Bonannella, C., Hengl, T., Heisig, J., Parente, L., Wright, M.N., Herold, M., de Bruin, S., 2022. Forest tree species distribution for Europe 2000-2020: mapping potential and realized distributions using spatiotemporal Machine Learning (preprint). In Review. https://doi.org/10.21203/rs.3.rs-1252972/v1

Bongers, F.J., Schmid, B., Bruelheide, H., Bongers, F., Li, S., von Oheimb, G., Li, Y., Cheng, A., Ma, K., Liu, X., 2021. Functional diversity effects on productivity increase with age in a forest biodiversity experiment. Nat. Ecol. Evol. 5, 1594–1603.

Boonman, C.C., Huijbregts, M.A., Benítez-López, A., Schipper, A.M., Thuiller, W., Santini, L., 2022. Trait-based projections of climate change effects on global biome distributions. Divers. Distrib. 28, 25–37.

Boonman, C.C.F., Benítez-López, A., Schipper, A.M., Thuiller, W., Anand, M., Cerabolini, B.E.L., Cornelissen, J.H.C., Gonzalez-Melo, A., Hattingh, W.N., Higuchi, P., Laughlin, D.C., Onipchenko, V.G., Peñuelas, J., Poorter, L., Soudzilovskaia, N.A., Huijbregts, M.A.J., Santini, L., 2020. Assessing the reliability of predicted plant trait distributions at the global scale. Glob. Ecol. Biogeogr. 29, 1034–1051. https://doi.org/10.1111/geb.13086

Bruelheide, H., Dengler, J., Jiménez-Alfaro, B., Purschke, O., Hennekens, S.M., Chytrý, M., Pillar, V.D., Jansen, F., Kattge, J., Sandel, B., Aubin, I., Biurrun, I., Field, R., Haider, S., Jandt, U., Lenoir, J., Peet, R.K., Peyre, G., Sabatini, F.M., Schmidt, M., Schrodt, F., Winter, M., Aćić, S., Agrillo, E., Alvarez, M., Ambarlı, D., Angelini, P., Apostolova, I., Arfin Khan, M.A.S., Arnst, E., Attorre, F., Baraloto, C., Beckmann, M., Berg, C., Bergeron, Y., Bergmeier, E., Bjorkman, A.D., Bondareva, V., Borchardt, P., Botta-Dukát, Z., Boyle, B., Breen, A., Brisse, H., Byun, C., Cabido, M.R., Casella, L.,

Cayuela, L., Černý, T., Chepinoga, V., Csiky, J., Curran, M., Ćušterevska, R., Dajić Stevanović, Z., De Bie, E., de Ruffray, P., De Sanctis, M., Dimopoulos, P., Dressler, S., Ejrnæs, R., El-Sheikh, M.A.E.M., Enquist, B., Ewald, J., Fagúndez, J., Finckh, M., Font, X., Forey, E., Fotiadis, G., García-Mijangos, I., Gasper, A.L., Golub, V., Gutierrez, A.G., Hatim, M.Z., He, T., Higuchi, P., Holubová, D., Hölzel, N., Homeier, J., Indreica, A., Işık Gürsoy, D., Jansen, S., Janssen, J., Jedrzejek, B., Jiroušek, M., Jürgens, N., Kącki, Z., Kavgacı, A., Kearsley, E., Kessler, M., Knollová, I., Kolomiychuk, V., Korolyuk, A., Kozhevnikova, M., Kozub, Ł., Krstonošić, D., Kühl, H., Kühn, I., Kuzemko, A., Küzmič, F., Landucci, F., Lee, M.T., Levesley, A., Li, C., Liu, H., Lopez-Gonzalez, G., Lysenko, T., Macanović, A., Mahdavi, P., Manning, P., Marcenò, C., Martynenko, V., Mencuccini, M., Minden, V., Moeslund, J.E., Moretti, M., Müller, J.V., Munzinger, J., Niinemets, Ü., Nobis, M., Noroozi, J., Nowak, A., Onyshchenko, V., Overbeck, G.E., Ozinga, W.A., Pauchard, A., Pedashenko, H., Peñuelas, J., Pérez-Haase, A., Peterka, T., Petřík, P., Phillips, O.L., Prokhorov, V., Rašomavičius, V., Revermann, R., Rodwell, J., Ruprecht, E., Rūsiņa, S., Samimi, C., Schaminée, J.H.J., Schmiedel, U., Šibík, J., Šilc, U., Škvorc, Ž., Smyth, A., Sop, T., Sopotlieva, D., Sparrow, B., Stančić, Z., Svenning, J., Swacha, G., Tang, Z., Tsiripidis, I., Turtureanu, P.D., Uğurlu, E., Uogintas, D., Valachovič, M., Vanselow, K.A., Vashenyak, Y., Vassilev, K., Vélez-Martin, E., Venanzoni, R., Vibrans, A.C., Violle, C., Virtanen, R., Wehrden, H., Wagner, V., Walker, D.A., Wana, D., Weiher, E., Wesche, K., Whitfeld, T., Willner, W., Wiser, S., Wohlgemuth, T., Yamalov, S., Zizka, G., Zverev, A., 2019. sPlot – A new tool for global vegetation analyses. J. Veg. Sci. 30, 161–186. https://doi.org/10.1111/jvs.12710

Bruelheide, H., Dengler, J., Purschke, O., Lenoir, J., Jiménez-Alfaro, B., Hennekens, S.M., Botta-Dukát, Z., Chytrý, M., Field, R., Jansen, F., Kattge, J., Pillar, V.D., Schrodt, F., Mahecha, M.D., Peet, R.K., Sandel, B., van Bodegom, P., Altman, J., Alvarez-Dávila, E., Arfin Khan, M.A.S., Attorre, F., Aubin, I., Baraloto, C., Barroso, J.G., Bauters, M., Bergmeier, E., Biurrun, I., Bjorkman, A.D., Blonder, B., Čarni, A., Cayuela, L., Černý, T., Cornelissen, J.H.C., Craven, D., Dainese, M., Derroire, G., De Sanctis, M., Díaz, S., Doležal, J., Farfan-Rios, W., Feldpausch, T.R., Fenton, N.J., Garnier, E., Guerin, G.R., Gutiérrez, A.G., Haider, S., Hattab, T., Henry, G., Hérault, B., Higuchi, P., Hölzel, N., Homeier, J., Jentsch, A., Jürgens, N., Kącki, Z., Karger, D.N., Kessler, M., Kleyer, M., Knollová, I., Korolyuk, A.Y., Kühn, I., Laughlin, D.C., Lens, F., Loos, J., Louault, F., Lyubenova, M.I., Malhi, Y., Marcenò, C., Mencuccini, M., Müller, J.V., Munzinger, J., Myers-Smith, I.H., Neill, D.A., Niinemets, Ü., Orwin, K.H., Ozinga, W.A., Penuelas, J., Pérez-Haase, A., Petřík, P., Phillips, O.L., Pärtel, M., Reich, P.B., Römermann, C., Rodrigues, A.V., Sabatini, F.M., Sardans, J., Schmidt, M., Seidler, G., Silva Espejo, J.E., Silveira, M., Smyth, A., Sporbert, M., Svenning, J.-C., Tang, Z., Thomas, R., Tsiripidis, I., Vassilev, K., Violle, C., Virtanen, R., Weiher, E., Welk, E., Wesche, K., Winter, M., Wirth, C., Jandt, U., 2018. Global trait–environment relationships of plant communities. Nat. Ecol. Evol. 2, 1906–1917. https://doi.org/10.1038/s41559-018-0699-8

Butler, E.E., Datta, A., Flores-Moreno, H., Chen, M., Wythers, K.R., Fazayeli, F., Banerjee, A., Atkin, O.K., Kattge, J., Amiaud, B., Blonder, B., Boenisch, G., Bond-Lamberty, B., Brown, K.A., Byun, C., Campetella, G., Cerabolini, B.E.L., Cornelissen, J.H.C., Craine, J.M., Craven, D., de Vries, F.T., Díaz, S., Domingues, T.F., Forey, E., González-Melo, A., Gross, N., Han, W., Hattingh, W.N., Hickler, T., Jansen, S., Kramer, K., Kraft, N.J.B., Kurokawa, H., Laughlin, D.C., Meir, P., Minden, V., Niinemets, Ü., Onoda, Y., Peñuelas, J., Read, Q., Sack, L., Schamp, B., Soudzilovskaia, N.A., Spasojevic, M.J., Sosinski, E., Thornton, P.E., Valladares, F., van Bodegom, P.M., Williams, M., Wirth, C., Reich, P.B., 2017. Mapping local and global variability in plant trait distributions. Proc. Natl. Acad. Sci. 114, E10937–E10946. https://doi.org/10.1073/pnas.1708984114

Butler, E.E., Wythers, K.R., Flores-Moreno, H., Ricciuto, D.M., Datta, A., Banerjee, A., Atkin, O.K., Kattge, J., Thornton, P.E., Anand, M., Burrascano, S., Byun, C., Cornelissen,

J.H.C., Forey, E., Jansen, S., Kramer, K., Minden, V., Reich, P.B., 2022. Increasing Functional Diversity in a Global Land Surface Model Illustrates Uncertainties Related to Parameter Simplification. J. Geophys. Res. Biogeosciences 127. https://doi.org/10.1029/2021JG006606

Chlus, A., Kruger, E.L., Townsend, P.A., 2020. Mapping three-dimensional variation in leaf mass per area with imaging spectroscopy and lidar in a temperate broadleaf forest. Remote Sens. Environ. 12.

Chlus, A., Townsend, P.A., 2022. Characterizing seasonal variation in foliar biochemistry with airborne imaging spectroscopy. Remote Sens. Environ. 275, 113023.

Congalton, R.G., Gu, J., Yadav, K., Thenkabail, P., Ozdogan, M., 2014. Global land cover mapping: A review and uncertainty analysis. Remote Sens. 6, 12070–12093.

Davrinche, A., Bittner, A., Bruelheide, H., Albert, G., Harpole, S., Haider, S., 2023. High within-tree leaf trait variation and its response to species diversity and soil nutrients (preprint). Ecology. https://doi.org/10.1101/2023.03.08.531739

Díaz, S., Kattge, J., Cornelissen, J.H.C., Wright, I.J., Lavorel, S., Dray, S., Reu, B., Kleyer, M., Wirth, C., Colin Prentice, I., Garnier, E., Bönisch, G., Westoby, M., Poorter, H., Reich, P.B., Moles, A.T., Dickie, J., Gillison, A.N., Zanne, A.E., Chave, J., Joseph Wright, S., Sheremet'ev, S.N., Jactel, H., Baraloto, C., Cerabolini, B., Pierce, S., Shipley, B., Kirkup, D., Casanoves, F., Joswig, J.S., Günther, A., Falczuk, V., Rüger, N., Mahecha, M.D., Gorné, L.D., 2016. The global spectrum of plant form and function. Nature 529, 167–171. https://doi.org/10.1038/nature16489

Díaz, S., Kattge, J., Cornelissen, J.H.C., Wright, I.J., Lavorel, S., Dray, S., Reu, B., Kleyer, M., Wirth, C., Colin Prentice, I., Garnier, E., Bönisch, G., Westoby, M., Poorter, H., Reich, P.B., Moles, A.T., Dickie, J., Gillison, A.N., Zanne, A.E., Chave, J., Joseph Wright, S., Sheremet'ev, S.N., Jactel, H., Baraloto, C., Cerabolini, B., Pierce, S., Shipley, B., Kirkup, D., Casanoves, F., Joswig, J.S., Günther, A., Falczuk, V., Rüger, N., Mahecha, M.D., Gorné, L.D., 2015. The global spectrum of plant form and function. Nature 529, 167–171. https://doi.org/10.1038/nature16489

Dong, N., Dechant, B., Wang, H., Wright, I.J., Prentice, I.C., 2023. Global leaf-trait mapping based on optimality theory. Glob. Ecol. Biogeogr. https://doi.org/10.1111/geb.13680

Ellsworth, D.S., Reich, P.B., 1993. Canopy structure and vertical patterns of photosynthesis and related leaf traits in a deciduous forest. Oecologia 96, 169–178.

Evans, J., Poorter, H., 2001. Photosynthetic acclimation of plants to growth irradiance: the relative importance of specific leaf area and nitrogen partitioning in maximizing carbon gain. Plant Cell Environ. 24, 755–767.

Friedl, M.A., McIver, D.K., Hodges, J.C.F., Zhang, X.Y., Muchoney, D., Strahler, A.H., Woodcock, C.E., Gopal, S., Schneider, A., Cooper, A., Baccini, A., Gao, F., Schaaf, C., 2002. Global land cover mapping from MODIS: algorithms and early results. Remote Sens. Environ. 83, 287–302. https://doi.org/10.1016/S0034-4257(02)00078-0

Fyllas, N.M., Michelaki, C., Galanidis, A., Evangelou, E., Zaragoza-Castells, J., Dimitrakopoulos, P.G., Tsadilas, C., Arianoutsou, M., Lloyd, J., 2020. Functional Trait Variation Among and Within Species and Plant Functional Types in Mountainous Mediterranean Forests. Front. Plant Sci. 11, 212. https://doi.org/10.3389/fpls.2020.00212

Garnier, E., Cortez, J., Billès, G., Navas, M.-L., Roumet, C., Debussche, M., Laurent, G., Blanchard, A., Aubry, D., Bellmann, A., Neill, C., Toussaint, J.-P., 2004. PLANT FUNCTIONAL MARKERS CAPTURE ECOSYSTEM PROPERTIES DURING SECONDARY SUCCESSION. Ecology 85, 2630–2637. https://doi.org/10.1890/03-0799

Guerin, G.R., Gallagher, R.V., Wright, I.J., Andrew, S.C., Falster, D.S., Wenk, E., Munroe, S.E.M., Lowe, A.J., Sparrow, B., 2022. Environmental associations of abundance-weighted functional traits in Australian plant communities. Basic Appl. Ecol. 58, 98–109. https://doi.org/10.1016/j.baae.2021.11.008

Harper, K.L., Lamarche, C., Hartley, A., Peylin, P., Ottlé, C., Bastrikov, V., San Martín, R., Bohnenstengel, S.I., Kirches, G., Boettcher, M., Shevchuk, R., Brockmann, C., Defourny, P., 2023. A 29-year time series of annual 300 m resolution plant-functional-type maps for climate models. Earth Syst. Sci. Data 15, 1465–1499. https://doi.org/10.5194/essd-15-1465-2023

Hijmans, R.J., 2022. raster: Geographic Data Analysis and Modeling. R package version 3.5-15. R Package.

Hijmans, R.J., Van Etten, J., Cheng, J., Mattiuzzi, M., Sumner, M., Greenberg, J.A., Lamigueiro, O.P., Bevan, A., Racine, E.B., Shortridge, A., 2015. Package 'raster.' R Package.

Hikosaka, K., Kumagai, T., Ito, A., 2016. Modeling canopy photosynthesis. Canopy Photosynth. Basics Appl. 239–268.

Houborg, R., McCabe, M.F., 2018. A Cubesat enabled Spatio-Temporal Enhancement Method (CESTEM) utilizing Planet, Landsat and MODIS data. Remote Sens. Environ. 209, 211–226. https://doi.org/10.1016/j.rse.2018.02.067

Hufkens, K., Bogaert, J., Dong, Q.H., Lu, L., Huang, C.L., Ma, M.G., Che, T., Li, X., Veroustraete, F., Ceulemans, R., 2008. Impacts and uncertainties of upscaling of remote-sensing data validation for a semi-arid woodland. J. Arid Environ. 72, 1490–1505. https://doi.org/10.1016/j.jaridenv.2008.02.012

Jetz, W., Cavender-Bares, J., Pavlick, R., Schimel, D., Davis, F.W., Asner, G.P., Guralnick, R., Kattge, J., Latimer, A.M., Moorcroft, P., Schaepman, M.E., Schildhauer, M.P., Schneider, F.D., Schrodt, F., Stahl, U., Ustin, S.L., 2016. Monitoring plant functional diversity from space. Nat. Plants 2, 16024. https://doi.org/10.1038/nplants.2016.24

Kambach, S., Sabatini, F.M., Attorre, F., Biurrun, I., Boenisch, G., Bonari, G., Čarni, A., Carranza, M.L., Chiarucci, A., Chytrý, M., Dengler, J., Garbolino, E., Golub, V., Güler, B., Jandt, U., Jansen, J., Jašková, A., Jiménez-Alfaro, B., Karger, D.N., Kattge, J., Knollová, I., Midolo, G., Moeslund, J.E., Pielech, R., Rašomavičius, V., Rūsiņa, S., Šibík, J., Stančić, Z., Stanisci, A., Svenning, J.-C., Yamalov, S., Zimmermann, N.E., Bruelheide, H., 2023. Climate-trait relationships exhibit strong habitat specificity in plant communities across Europe. Nat. Commun. 14, 712. https://doi.org/10.1038/s41467-023-36240-6

Kattge, J., Bönisch, G., Díaz, S., Lavorel, S., Prentice, I.C., Leadley, P., Tautenhahn, S., Werner, G.D., Aakala, T., Abedi, M., 2020. TRY plant trait database–enhanced coverage and open access. Glob. Change Biol. 26, 119–188.

Kattge, J., DíAz, S., Lavorel, S., Prentice, I.C., Leadley, P., BöNisch, G., Garnier, E., Westoby, M., Reich, P.B., Wright, I.J., Cornelissen, J.H.C., Violle, C., Harrison, S.P., Van BODEGOM, P.M., Reichstein, M., Enquist, B.J., Soudzilovskaia, N.A., Ackerly, D.D., Anand, M., Atkin, O., Bahn, M., Baker, T.R., Baldocchi, D., Bekker, R., Blanco, C.C., Blonder, B., Bond, W.J., Bradstock, R., Bunker, D.E., Casanoves, F., Cavender-Bares, J., Chambers, J.Q., Chapin Iii, F.S., Chave, J., Coomes, D., Cornwell, W.K., Craine, J.M., Dobrin, B.H., Duarte, L., Durka, W., Elser, J., Esser, G., Estiarte, M., Fagan, W.F., Fang, J., FernáNdez-MéNdez, F., Fidelis, A., Finegan, B., Flores, O., Ford, H., Frank, D., Freschet, G.T., Fyllas, N.M., Gallagher, R.V., Green, W.A., Gutierrez, A.G., Hickler, T., Higgins, S.I., Hodgson, J.G., Jalili, A., Jansen, S., Joly, C.A., Kerkhoff, A.J., Kirkup, D., Kitajima, K., Kleyer, M., Klotz, S., Knops, J.M.H., Kramer, K., KüHn, I., Kurokawa, H., Laughlin, D., Lee, T.D., Leishman, M., Lens, F., Lenz, T., Lewis, S.L., Lloyd, J., Llusià, J., Louault, F., Ma, S., Mahecha, M.D., Manning, P., Massad, T., Medlyn, B.E., Messier, J., Moles, A.T., MüLler, S.C., Nadrowski, K., Naeem, S., Niinemets, ü., NöLlert, S., NüSke, A., Ogaya, R., Oleksyn, J., Onipchenko, V.G., Onoda, Y., OrdoñEz, J., Overbeck, G., Ozinga, W.A., PatiñO, S., Paula, S., Pausas, J.G., PeñUelas, J., Phillips, O.L., Pillar, V., Poorter, H., Poorter, L., Poschlod, P., Prinzing, A., Proulx, R., Rammig, A., Reinsch, S., Reu, B., Sack, L., Salgado-Negret, B., Sardans, J., Shiodera, S., Shipley, B., Siefert, A., Sosinski, E., Soussana, J.-F., Swaine, E., Swenson, N., Thompson, K., Thornton, P., Waldram, M., Weiher, E., White, M., White, S., Wright, S.J., Yguel, B., Zaehle, S.,

Zanne, A.E., Wirth, C., 2011. TRY - a global database of plant traits. Glob. Change Biol. 17, 2905–2935. https://doi.org/10.1111/j.1365-2486.2011.02451.x
Kattge, J., Knorr, W., Raddatz, T., Wirth, C., 2009. Quantifying photosynthetic capacity and its relationship to leaf nitrogen content for global-scale terrestrial biosphere models. Glob. Change Biol. 15, 976–991. https://doi.org/10.1111/j.1365-2486.2008.01744.x
Lang, N., Kalischek, N., Armston, J., Schindler, K., Dubayah, R., Wegner, J.D., 2022. Global canopy height regression and uncertainty estimation from GEDI LIDAR waveforms with deep ensembles. Remote Sens. Environ. 268, 112760. https://doi.org/10.1016/j.rse.2021.112760
Lawrence, P.J., Chase, T.N., 2007. Representing a new MODIS consistent land surface in the Community Land Model (CLM 3.0). J. Geophys. Res. 112, G01023. https://doi.org/10.1029/2006JG000168
Loozen, Y., Rebel, K.T., de Jong, S.M., Lu, M., Ollinger, S.V., Wassen, M.J., Karssenberg, D., 2020. Mapping canopy nitrogen in European forests using remote sensing and environmental variables with the random forests method. Remote Sens. Environ. 247, 111933. https://doi.org/10.1016/j.rse.2020.111933
Loveland, T.R., Belward, A.S., 1997. The IGBP-DIS global 1km land cover data set, DISCover: First results. Int. J. Remote Sens. 18, 3289–3295. https://doi.org/10.1080/014311697217099
Macander, M.J., Nelson, P.R., Nawrocki, T.W., Frost, G.V., Orndahl, K.M., Palm, E.C., Wells, A.F., Goetz, S.J., 2022. Time-series maps reveal widespread change in plant functional type cover across Arctic and boreal Alaska and Yukon. Environ. Res. Lett. 17, 054042. https://doi.org/10.1088/1748-9326/ac6965
Madani, N., Kimball, J.S., Ballantyne, A.P., Affleck, D.L.R., van Bodegom, P.M., Reich, P.B., Kattge, J., Sala, A., Nazeri, M., Jones, M.O., Zhao, M., Running, S.W., 2018. Future global productivity will be affected by plant trait response to climate. Sci. Rep. 8, 2870. https://doi.org/10.1038/s41598-018-21172-9
Maynard, D.S., Bialic-Murphy, L., Zohner, C.M., Averill, C., van den Hoogen, J., Ma, H., Mo, L., Smith, G.R., Acosta, A.T.R., Aubin, I., Berenguer, E., Boonman, C.C.F., Catford, J.A., Cerabolini, B.E.L., Dias, A.S., González-Melo, A., Hietz, P., Lusk, C.H., Mori, A.S., Niinemets, Ü., Pillar, V.D., Pinho, B.X., Rosell, J.A., Schurr, F.M., Sheremetev, S.N., da Silva, A.C., Sosinski, Ê., van Bodegom, P.M., Weiher, E., Bönisch, G., Kattge, J., Crowther, T.W., 2022. Global relationships in tree functional traits. Nat. Commun. 13, 3185. https://doi.org/10.1038/s41467-022-30888-2
Meyer, H., Pebesma, E., 2021. Predicting into unknown space? Estimating the area of applicability of spatial prediction models. Methods Ecol. Evol. 12, 1620–1633. https://doi.org/10.1111/2041-210X.13650
Moreno-Martínez, Á., Camps-Valls, G., Kattge, J., Robinson, N., Reichstein, M., van Bodegom, P., Kramer, K., Cornelissen, J.H.C., Reich, P., Bahn, M., Niinemets, Ü., Peñuelas, J., Craine, J.M., Cerabolini, B.E.L., Minden, V., Laughlin, D.C., Sack, L., Allred, B., Baraloto, C., Byun, C., Soudzilovskaia, N.A., Running, S.W., 2018. A methodology to derive global maps of leaf traits using remote sensing and climate data. Remote Sens. Environ. 218, 69–88. https://doi.org/10.1016/j.rse.2018.09.006
Mugabowindekwe, M., Brandt, M., Chave, J., Reiner, F., Skole, D.L., Kariryaa, A., Igel, C., Hiernaux, P., Ciais, P., Mertz, O., 2022. Nation-wide mapping of tree-level aboveground carbon stocks in Rwanda. Nat. Clim. Change 1–7.
Musavi, T., Mahecha, M.D., Migliavacca, M., Reichstein, M., Van De Weg, M.J., Van Bodegom, P.M., Bahn, M., Wirth, C., Reich, P.B., Schrodt, F., Kattge, J., 2015. The imprint of plants on ecosystem functioning: A data-driven approach. Int. J. Appl. Earth Obs. Geoinformation 43, 119–131. https://doi.org/10.1016/j.jag.2015.05.009
Ploton, P., Mortier, F., Réjou-Méchain, M., Barbier, N., Picard, N., Rossi, V., Dormann, C., Cornu, G., Viennois, G., Bayol, N., Lyapustin, A., Gourlet-Fleury, S., Pélissier, R., 2020. Spatial validation reveals poor predictive performance of large-scale ecological mapping models. Nat. Commun. 11, 4540. https://doi.org/10.1038/s41467-020-18321-y

Potapov, P., Li, X., Hernandez-Serna, A., Tyukavina, A., Hansen, M.C., Kommareddy, A., Pickens, A., Turubanova, S., Tang, H., Silva, C.E., Armston, J., Dubayah, R., Blair, J.B., Hofton, M., 2021. Mapping global forest canopy height through integration of GEDI and Landsat data. Remote Sens. Environ. 253, 112165. https://doi.org/10.1016/j.rse.2020.112165

Poulter, B., MacBean, N., Hartley, A., Khlystova, I., Arino, O., Betts, R., Bontemps, S., Boettcher, M., Brockmann, C., Defourny, P., Hagemann, S., Herold, M., Kirches, G., Lamarche, C., Lederer, D., Ottlé, C., Peters, M., Peylin, P., 2015. Plant functional type classification for earth system models: results from the European Space Agency's Land Cover Climate Change Initiative. Geosci. Model Dev. 8, 2315–2328. https://doi.org/10.5194/gmd-8-2315-2015

Reich, P.B., 2014. The world-wide 'fast-slow' plant economics spectrum: a traits manifesto. J. Ecol. 102, 275–301. https://doi.org/10.1111/1365-2745.12211

Reich, P.B., Wright, I.J., Lusk, C.H., 2007. PREDICTING LEAF PHYSIOLOGY FROM SIMPLE PLANT AND CLIMATE ATTRIBUTES: A GLOBAL GLOPNET ANALYSIS. Ecol. Appl. 17, 1982–1988. https://doi.org/10.1890/06-1803.1

Sabatini, F.M., Lenoir, J., Hattab, T., Arnst, E.A., Chytrý, M., Dengler, J., Ruffray, P.D., Hennekens, S.M., Jandt, U., Jansen, F., Jiménez, B., Kattge, J., Levesley, A., Pillar, V.D., Purschke, O., Sandel, B., Sultana, F., Aavik, T., Aćić, S., Acosta, A.T.R., Agrillo, E., Alvarez, M., Apostolova, I., Aubin, I., Banerjee, A., Bauters, M., Bergeron, Y., Bergmeier, E., Biurrun, I., Bjorkman, A.D., Bonari, G., Bondareva, V., Brunet, J., Čarni, A., Casella, L., Cayuela, L., Černý, T., Chepinoga, V., Csiky, J., Ćušterevska, R., Bie, E.D., de Gasper, A.L., Sanctis, M.D., Dimopoulos, P., Dolezal, J., Dziuba, T., El, M.A., El, R.M., Enquist, B., Ewald, J., Fazayeli, F., Field, R., Finckh, M., Gachet, S., Galán, A., Garbolino, E., Gholizadeh, H., Giorgis, M., Golub, V., Alsos, I.G., Grytnes, A., Guerin, G.R., Gutiérrez, A.G., Haider, S., Hatim, M.Z., Hérault, B., Mendoza, G.H., Hölzel, N., Homeier, J., Hubau, W., Indreica, A., Janssen, J.A.M., Jedrzejek, B., Jentsch, A., Jürgens, N., Kącki, Z., Kapfer, J., Karger, D.N., Kavgacı, A., Kearsley, E., Kessler, M., Khanina, L., Killeen, T., Korolyuk, A., Kreft, H., Kühl, H.S., Kuzemko, A., Landucci, F., Lengyel, A., Lens, F., Lingner, D.V., Liu, H., Lysenko, T., Mahecha, M.D., Marcenò, C., Martynenko, V., Moeslund, J.E., Mendoza, A.M., 2021. sPlotOpen – An environmentally balanced, open-access, global dataset of vegetation plots. Glob. Ecol. Biogeogr. 00, 1–25. https://doi.org/10.1111/geb.13346

Scheiter, S., Langan, L., Higgins, S.I., 2013. Next-generation dynamic global vegetation models: learning from community ecology. New Phytol. 198, 957–969.

Schiller, C., Schmidtlein, S., Boonman, C., Moreno-Martínez, A., Kattenborn, T., 2021. Deep learning and citizen science enable automated plant trait predictions from photographs. Sci. Rep. 11, 16395. https://doi.org/10.1038/s41598-021-95616-0

Shi, Y., Wang, J., Qin, J., Qu, Y., 2015. An Upscaling Algorithm to Obtain the Representative Ground Truth of LAI Time Series in Heterogeneous Land Surface. Remote Sens. 7, 12887–12908. https://doi.org/10.3390/rs71012887

Simard, M., Pinto, N., Fisher, J.B., Baccini, A., 2011. Mapping forest canopy height globally with spaceborne lidar. J. Geophys. Res. 116, G04021. https://doi.org/10.1029/2011JG001708

Šímová, I., Violle, C., Svenning, J.-C., Kattge, J., Engemann, K., Sandel, B., Peet, R.K., Wiser, S.K., Blonder, B., McGill, B.J., Boyle, B., Morueta-Holme, N., Kraft, N.J.B., van Bodegom, P.M., Gutiérrez, A.G., Bahn, M., Ozinga, W.A., Tószögyová, A., Enquist, B.J., 2018. Spatial patterns and climate relationships of major plant traits in the New World differ between woody and herbaceous species. J. Biogeogr. 45, 895–916. https://doi.org/10.1111/jbi.13171

Soetart, K., Van den Meersche, K., van Oevelen, D., 2022. limSolve: Solving Linear Inverse Models. R package version 1.5.1. R Package.

Swenson, N.G., Weiser, M.D., 2010. Plant geography upon the basis of functional traits: an example from eastern North American trees. Ecology 91, 2234–2241. https://doi.org/10.1890/09-1743.1
Vallicrosa, H., Sardans, J., Janssens, I.A., Penuelas, J., 2021. Global maps and factors driving forest foliar elemental composition: the importance of genetic legacy. New Phytol.
Vallicrosa, H., Sardans, J., Maspons, J., Peñuelas, J., 2022. Global distribution and drivers of forest biome foliar nitrogen to phosphorus ratios (N:P). Glob. Ecol. Biogeogr. 31, 861–871. https://doi.org/10.1111/geb.13457
van Bodegom, P.M., Douma, J.C., Verheijen, L.M., 2014. A fully traits-based approach to modeling global vegetation distribution. Proc. Natl. Acad. Sci. 111, 13733–13738. https://doi.org/10.1073/pnas.1304551110
Van Bodegom, P.M., Douma, J.C., Witte, J.P.M., Ordoñez, J.C., Bartholomeus, R.P., Aerts, R., 2012. Going beyond limitations of plant functional types when predicting global ecosystem-atmosphere fluxes: exploring the merits of traits-based approaches: Merits of traits-based vegetation modelling. Glob. Ecol. Biogeogr. 21, 625–636. https://doi.org/10.1111/j.1466-8238.2011.00717.x
Van den Meersche, K., Soetaert, K., Van Oevelen, D., 2009. xsample (): an R function for sampling linear inverse problems. J. Stat. Softw. 30, 1–15.
Walker, A.P., Beckerman, A.P., Gu, L., Kattge, J., Cernusak, L.A., Domingues, T.F., Scales, J.C., Wohlfahrt, G., Wullschleger, S.D., Woodward, F.I., 2014. The relationship of leaf photosynthetic traits - V_{cmax} and J_{max} - to leaf nitrogen, leaf phosphorus, and specific leaf area: a meta-analysis and modeling study. Ecol. Evol. 4, 3218–3235. https://doi.org/10.1002/ece3.1173
Walker, A.P., Quaife, T., van Bodegom, P.M., De Kauwe, M.G., Keenan, T.F., Joiner, J., Lomas, M.R., MacBean, N., Xu, C., Yang, X., Woodward, F.I., 2017. The impact of alternative trait-scaling hypotheses for the maximum photosynthetic carboxylation rate (V_{cmax}) on global gross primary production. New Phytol. 215, 1370–1386. https://doi.org/10.1111/nph.14623
Wang, H., Harrison, S.P., Li, M., Prentice, I.C., Qiao, S., Wang, R., Xu, H., Mengoli, G., Peng, Y., Yang, Y., 2022. The China plant trait database version 2. Sci. Data 9, 769. https://doi.org/10.1038/s41597-022-01884-4
Wang, L., Arora, V.K., Bartlett, P., Chan, E., Curasi, S.R., 2022. Mapping of ESA-CCI land cover data to plant functional types for use in the CLASSIC land model (preprint). Biogeochemistry: Modelling, Terrestrial. https://doi.org/10.5194/egusphere-2022-923
Wang, W., Fan, Y., Li, Y., Li, X., Tang, S., 2023. An Individual Tree Segmentation Method from Mobile Mapping Point Clouds Based on Improved 3D Morphological Analysis. IEEE J. Sel. Top. Appl. Earth Obs. Remote Sens.
Wang, Y., Li, G., Ding, J., Guo, Z., Tang, S., Wang, C., Huang, Q., Liu, R., Chen, J.M., 2016. A combined GLAS and MODIS estimation of the global distribution of mean forest canopy height. Remote Sens. Environ. 174, 24–43. https://doi.org/10.1016/j.rse.2015.12.005
Wang, Z., Chlus, A., Geygan, R., Ye, Z., Zheng, T., Singh, A., Couture, J.J., Cavender-Bares, J., Kruger, E.L., Townsend, P.A., 2020. Foliar functional traits from imaging spectroscopy across biomes in eastern North America. New Phytol. nph.16711. https://doi.org/10.1111/nph.16711
Wolf, S., Mahecha, M.D., Sabatini, F.M., Wirth, C., Bruelheide, H., Kattge, J., Moreno Martínez, Á., Mora, K., Kattenborn, T., 2022. Citizen science plant observations encode global trait patterns. Nat. Ecol. Evol. https://doi.org/10.1038/s41559-022-01904-x
Wright, I.J., Reich, P.B., Cornelissen, J.H.C., Falster, D.S., Garnier, E., Hikosaka, K., Lamont, B.B., Lee, W., Oleksyn, J., Osada, N., Poorter, H., Villar, R., Warton, D.I., Westoby, M., 2005. Assessing the generality of global leaf trait relationships. New Phytol. 166, 485–496. https://doi.org/10.1111/j.1469-8137.2005.01349.x

Wright, I.J., Reich, P.B., Westoby, M., Ackerly, D.D., Baruch, Z., Bongers, F., Cavender-Bares, J., Chapin, T., Cornelissen, J.H.C., Diemer, M., Flexas, J., Garnier, E., Groom, P.K., Gulias, J., Hikosaka, K., Lamont, B.B., Lee, T., Lee, W., Lusk, C., Midgley, J.J., Navas, M.-L., 2004. The worldwide leaf economics spectrum 428, 7.

Yang, Y., Zhu, Q., Peng, C., Wang, H., Chen, H., 2015. From plant functional types to plant functional traits: A new paradigm in modelling global vegetation dynamics. Prog. Phys. Geogr. Earth Environ. 39, 514–535. https://doi.org/10.1177/0309133315582018

Yu, W., Li, J., Liu, Q., Zeng, Y., Zhao, J., Xu, B., Yin, G., 2018. Global Land Cover Heterogeneity Characteristics at Moderate Resolution for Mixed Pixel Modeling and Inversion. Remote Sens. 10, 856. https://doi.org/10.3390/rs10060856

Zeng, Y., Hao, D., Huete, A., Dechant, B., Berry, J., Chen, J.M., Joiner, J., Frankenberg, C., Bond-Lamberty, B., Ryu, Y., 2022. Optical vegetation indices for monitoring terrestrial ecosystems globally. Nat. Rev. Earth Environ. 3, 477–493.

Zhang, Y.-W., Guo, Y., Tang, Z., Feng, Y., Zhu, X., Xu, W., Bai, Y., Zhou, G., Xie, Z., Fang, J., 2021. Patterns of nitrogen and phosphorus pools in terrestrial ecosystems in China. Earth Syst. Sci. Data 13, 5337–5351. https://doi.org/10.5194/essd-13-5337-2021

Appendix A. Details for methods to quantify trait variations within PFTs.

Heterogeneity filtering. For this approach, we combined the PFT-mean trait values with global maps of LCT cover fractions for each grid cell, both provided by Butler and originally based on the TRY database (Kattge et al., 2020, 2011) and MODIS and AVHRR satellite products of land cover (Lawrence and Chase, 2007). For each 0.5° grid cell, we then estimated the trait variability by calculating the coefficient of variation (CV) of a variable in which each PFT mean trait value was represented proportional to its LCT cover fraction (Fig. A1). For each trait, we categorized grid cells with higher CV than the median of all grid cells as 'heterogeneous' and those with lower CV than the median as 'homogeneous'.

Unmixing. This approach entails essentially reverse engineering the final step of calculating grid-cell averages weighted by LCT cover in the generation of some of the 'PFT+Env' trait maps (Fig. 1). While not all maps applied the LCT weighting after the spatialization, this approach can be applied to all maps as the only assumption is the linear mixing of LCTs, i.e. only the spatial distribution of LCT cover is used. The unmixing was done by using a three by three grid cell moving window within which the system of overdetermined linear equations for six PFTs (ENF, DNF, EBF, DBF, SHR, GRA) was solved. For each grid-cell, there is one linear equation that equates the final grid cell trait value (known) with the sum over the six products of fractional LCT cover (known) times the corresponding local, PFT-specific trait value (unknown). For solving the linear equation systems the function *lsei* of the R package *limSolve* was used in combination with the *focal* function of the *terra* package (Hijmans et al., 2015; Soetart et al., 2022; Van den Meersche et al., 2009). We evaluated the performance of the unmixing approach with the categorical ('PFT') maps provided by Butler and found that it performed robustly for ENF and DNF, and reasonably well for DBF and EBF but could not be used for SHR and GRA (Fig. A2a). The limitations for SHR and GRA are likely due to their broad trait distributions and their co-occurrence with other LCTs with similar trait values. To exclude grid cells where the unmixing method did not work well, we applied a threshold on the fractional cover of the relevant PFT of 5% and applied thresholds on the maximum and minimum possible trait values to exclude large outliers or ecologically implausible values. Even after this filtering step, considerably more data were left for analyses of ENF and DBF than in case of applying the heterogeneity filtering approach.

Overall approach. Due to the limitations of both approaches for some LCTs, we combined the unmixing approach for ENF, DBF, and EBF with the heterogeneity filtering approach for SHR and GRA. For EBF, we chose unmixing as it provided better coverage.

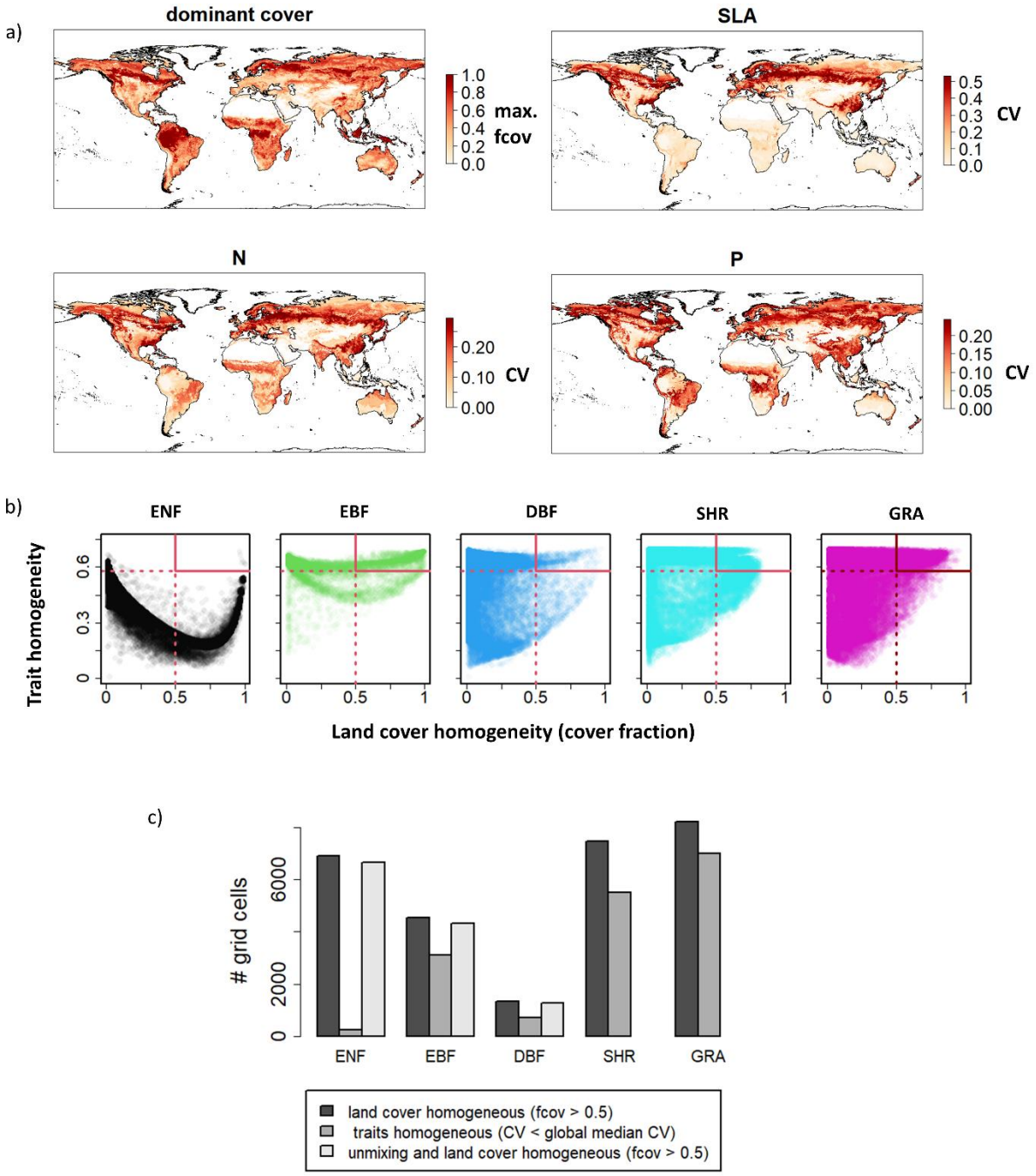

Figure A1: Overview of estimated within grid cell trait variability and its relationship with land cover homogeneity. a) estimates of within grid cell coefficient of variation maps are shown for each trait. For reference, the maximum fractional cover over all landcover types in a given grid cell (´dominant cover´) is shown. b) relationships between the within-grid-cell trait homogeneity (0.7-CV) vs. land cover homogeneity (cover fraction) per land cover type for SLA. Thresholds on both axes illustrate which data would remain (upper right hand corner with continuous red lines) after such a selection based on a minimum of 50% cover and a level of homogeneity exceeding the global median. c) overview of impact on the land cover and trait homogeneity thresholds on remaining vegetated grid cells at the global scale

together with unmixing results (for SLA). Note that unmixing results can be used also at lower cover thresholds. In c) the bar for the ´traits homogeneous´ category was slightly increased to make it visible.

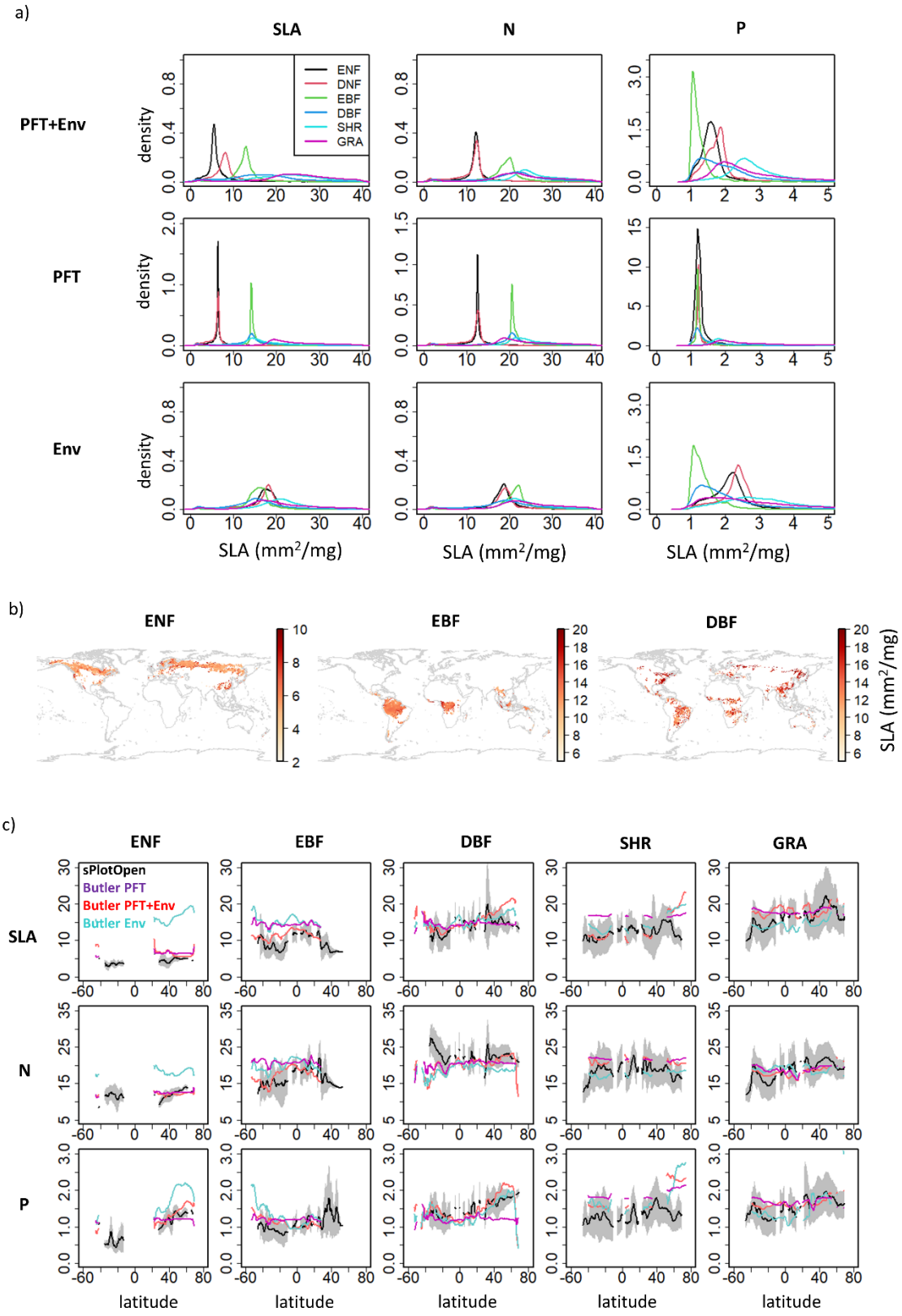

Figure A2: Unmixing results based on different versions of the Butler maps. The categorical case ('PFT') can serve as a reference as for each PFT one to three discrete values were assigned. a) trait

distributions from unmixing. b) unmixed PFT maps for Butler PFT+Env for SLA. c) comparison of combined unmixing/heterogeneity filtering to sPlotOpen TWM reference data.

Appendix B. Overview of all individual upscaled maps

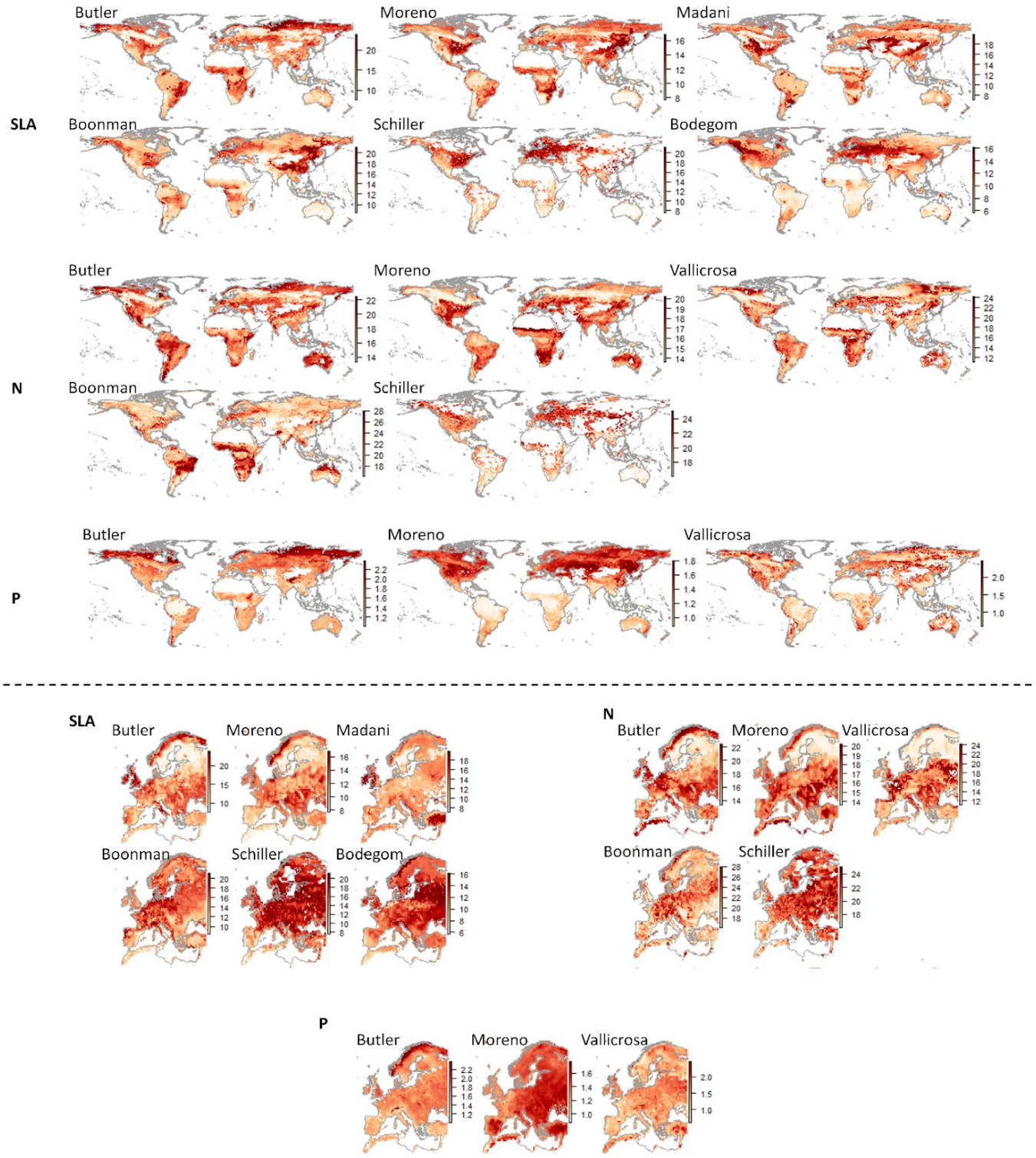

Figure B1: Overview of all individual upscaled maps for SLA, N and P. Units are as in Fig. 5. As the maps have both different mean values and levels of variability, each map is shown with a different scale

in order to facilitate the comparison of spatial patterns. Global maps are shown on top of the horizontal dashed line, detail maps of Europe are shown below the line. For each trait, the top row for shows maps based on PFT+Env upscaling approaches, the bottom rows maps based on Env upscaling approaches.